QEX

March/April 2021

www.arrl.org

A Forum for Communications Experimenters

Issue No. 325

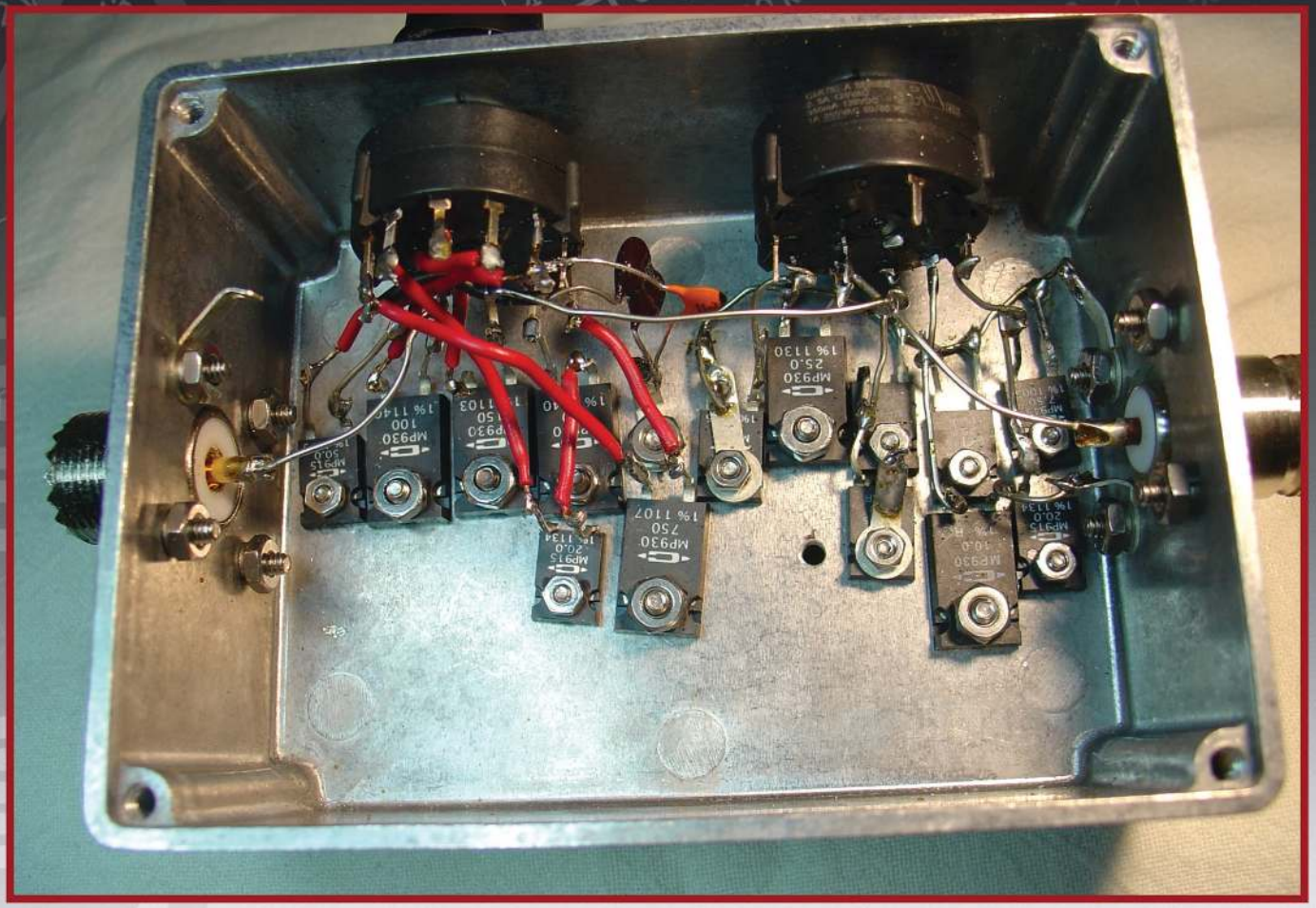

AD5X designs a test box for measuring antenna tuner losses.

Peerless Pathfinder

With Kenwood's advanced TM-D710G you can harness today's most exciting developments in radio communications, including EchoLink®, AX.25, and the latest features of APRS®.

- Built-in 1200/9600 bps packet TNC
- High RF Power Output (50W)
- Dual Receive
- 1000 Multifunction Memory Channels
- Multiple Scan & Visual Scan
- Switchable Amber/Green Backlit LCD
- Weather Alert/RX
- Voice Guidance & Storage Option

The control head is detached and comes with remote cable for easy installation. The TM-D710G is a true dual-band operation radio so VHF+VHF/VHF+UHF/UHF+UHF operation is possible.

TM-D710G

DATA COMMUNICATOR 144/440MHz FM Dual Bander

APRS® is a registered trademark of Bob Bruninga. see www.aprs.org
EchoLink® is a registered trademark of Synergenics, LLC in the USA. see www.echolink.org

KENWOOD

Customer Support: (310) 639-4200
Fax: (310) 537-8235

www.kenwoodusa.com

ISO9001 Registered

ADS#00221

QEX

QEX (ISSN: 0886-8093) is published bimonthly in January, March, May, July, September, and November by the American Radio Relay League, 225 Main St., Newington, CT 06111-1400. Periodicals postage paid at Hartford, CT and at additional mailing offices.

POSTMASTER: Send address changes to: QEX, 225 Main St., Newington, CT 06111-1400
Issue No. 325

Publisher
American Radio Relay League

Kazimierz "Kai" Siwiak, KE4PT
Editor

Lori Weinberg, KB1EIB
Assistant Editor

Scotty Cowling, WA2DFI
Ray Mack, W5IFS
Contributing Editors

Production Department

Becky R. Schoenfeld, W1BXY
Publications Manager

Michelle Bloom, WB1ENT
Production Supervisor

David Pingree, N1NAS
Senior Technical Illustrator

Brian Washing
Technical Illustrator

Advertising Information

Janet L. Rocco, W1JLR
Business Services
860-594-0203 – Direct
800-243-7768 – ARRL
860-594-4285 – Fax

Circulation Department

Cathy Stepina
QEX Circulation

Offices

225 Main St., Newington, CT 06111-1400 USA
Telephone: 860-594-0200
Fax: 860-594-0259 (24-hour direct line)
Email: **qex@arrl.org**

Subscription rate for 6 print issues:

In the US: $29

US by First Class Mail: $40;

International and Canada by Airmail: $35

ARRL members receive the digital edition of *QEX* as a member benefit.

In order to ensure prompt delivery, we ask that you periodically check the address information on your mailing label. If you find any inaccuracies, please contact the Circulation Department immediately. Thank you for your assistance.

March/April 2021

About the Cover

Phil Salas, AD5X, designed and built a test box for measuring losses in antenna tuners. The test box presents different loads to the antenna tuner, covering a range of SWRs from 1:1 to 10:1 for low impedances and between 1:1 and 16:1 for high impedances. A duplicate test box is used by the ARRL lab for their antenna tuner loss tests.

In This Issue

Index of Advertisers

The American Radio Relay League

The American Radio Relay League, Inc, is a noncommercial association of radio amateurs, organized for the promotion of interest in Amateur Radio communication and experimentation, for the establishment of networks to provide communications in the event of disasters or other emergencies, for the advancement of the radio art and of the public welfare, for the representation of the radio amateur in legislative matters, and for the maintenance of fraternalism and a high standard of conduct.

ARRL is an incorporated association without capital stock chartered under the laws of the state of Connecticut, and is an exempt organization under Section 501(c)(3) of the Internal Revenue Code of 1986. Its affairs are governed by a Board of Directors, whose voting members are elected every three years by the general membership. The officers are elected or appointed by the Directors. The League is noncommercial, and no one who could gain financially from the shaping of its affairs is eligible for membership on its Board.

"Of, by, and for the radio amateur," ARRL numbers within its ranks the vast majority of active amateurs in the nation and has a proud history of achievement as the standard-bearer in amateur affairs.

A *bona fide* interest in Amateur Radio is the only essential qualification of membership; an Amateur Radio license is not a prerequisite, although full voting membership is granted only to licensed amateurs in the US.

Membership inquiries and general correspondence should be addressed to the administrative headquarters:

ARRL
225 Main St.
Newington, CT 06111 USA
Telephone: 860-594-0200
FAX: 860-594-0259 (24-hour direct line)

Officers

President: Rick Roderick, K5UR
P.O. Box 1463, Little Rock, AR 72203

The purpose of *QEX* is to:

1) provide a medium for the exchange of ideas and information among Amateur Radio experimenters,

2) document advanced technical work in the Amateur Radio field, and

3) support efforts to advance the state of the Amateur Radio art.

All correspondence concerning *QEX* should be addressed to the American Radio Relay League, 225 Main St., Newington, CT 06111 USA. Envelopes containing manuscripts and letters for publication in *QEX* should be marked Editor, *QEX*.

Both theoretical and practical technical articles are welcomed. Manuscripts should be submitted in word-processor format, if possible. We can redraw any figures as long as their content is clear. Photos should be glossy, color or black-and-white prints of at least the size they are to appear in *QEX* or high-resolution digital images (300 dots per inch or higher at the printed size). Further information for authors can be found on the Web at **www.arrl.org/qex/** or by e-mail to **qex@arrl.org**.

Any opinions expressed in *QEX* are those of the authors, not necessarily those of the Editor or the League. While we strive to ensure all material is technically correct, authors are expected to defend their own assertions. Products mentioned are included for your information only; no endorsement is implied. Readers are cautioned to verify the availability of products before sending money to vendors.

Kazimierz "Kai" Siwiak, KE4PT

Perspectives

Making Waves Historically

A historical perspective helps us better understand our radio arts. Radio receivers, transmitters and related devices all went through phases, starting out as purely mechanical-electrical devices. They progressed through vacuum tube electronics, and migrated to semiconductors and integrated circuits. Today's receivers and transmitters are ever more reliant on digital implementations with software defined functions replacing physical circuits. One can well imagine the analog-to-digital and digital-to-analog direct sampling of signals right at the terminals of an antenna. In fact such implementations have been built! Their historical perspective was one of evolution from mechanical-electrical devices to software driven solutions.

Antennas and propagation of course have escaped digitization. We've noted before that the very first technical article in the premier December 1915 issue of *QST* was "Pictured Electro-Magnetic Waves," by Clarence D. Tuska, the co-founder of the ARRL. More than a century later we still map radiation patterns, but with ever more precision using modern simulation tools. The tools went digital. Not long after Tuska's article, Professors Hidetsugu Yagi and Shintaro Uda described their classic Yagi-Uda directional array antenna in 1926. It has since become one of the most popular antenna configurations, along with the half-wave dipole and the vertical antenna. We celebrate the Yagi-Uda array by reprinting the original article in these pages. The antenna originated in the 1920s, but its basic form remains the same. Its experimental and mathematical analysis continues to this day, bringing us extensions and versions optimized for various performance parameters.

Keep your perspective historical!

In This Issue

Hidetsugu Yagi and Shintaro Uda describe the classic Yagi-Uda array antenna in this reprint of their 1926 article.

Robert J. Zavrel, W7SX, extends the Yagi-Uda array concept to the "W7SX Array" by not restricting element lengths to a half wavelength.

Jerry Spring, VE6TL, discusses the onset of Solar Cycle 25 and the MG II index.

Eric Nichols, KL7AJ, in his Essay Series, discusses electro-mechanical devices and control theory.

Phil Salas, AD5X, describes his method and fixtures for measuring antenna tuner loss.

Kai Siwiak, KE4PT, describes lightning-induced electromagnetic pulse effects.

Peter DeNeef, AE7PD, addresses RF exposure from a 70 cm band collinear dipole array.

Writing for *QEX*

Please keep the full-length *QEX* articles flowing in, or share a **Technical Note** of several hundred words in length plus a figure or two. *QEX* is edited by Kazimierz "Kai" Siwiak, KE4PT, (**ksiwiak@arrl.org**) and is published bimonthly. *QEX* is a forum for the free exchange of ideas among communications experimenters. All members can access digital editions of all four ARRL magazines: *QST*, *On the Air, QEX*, and *NCJ* as a member benefit. The *QEX printed edition* annual subscription rate (6 issues per year) for members and non-members is $29 in the United States. First Class mail delivery in the US is available at an annual rate of $40. For international subscribers, including those in Canada and Mexico, *QEX* printed edition can be delivered by airmail for $35 annually, see **www.arrl.org/qex**.

Would you like to write for *QEX*? We pay $50 per published page for full articles and *QEX* Technical Notes. Get more information and an Author Guide at **www.arrl.org/qex-author-guide**. If you prefer postal mail, send a business-size self-addressed, stamped (US postage) envelope to: *QEX* Author Guide, c/o Maty Weinberg, ARRL, 225 Main St., Newington, CT 06111.

Very kindest regards, Kazimierz "Kai" Siwiak, KE4PT, *QEX* Editor

Phil Salas, AD5X

1517 Creekside Dr., Richardson, TX 75081; **ad5x@arrl.net**

Antenna Tuner Loss Measurements

Measure antenna tuner losses with this antenna tuner loss test box and method.

No antenna tuner is lossless, especially when matching impedances that are much higher or lower than normal. I've had the opportunity to test a number of automatic antenna tuners for *QST*, and so have come up with a standard antenna tuner loss test box. A duplicate test box is used by the ARRL lab for their antenna tuner loss tests.

Many antenna tuners specify a resistive matching range. While not representative of most actual impedances that are to be matched, pure resistances can give us a good reference set of tests by which all antenna tuners can be compared. To that end, I developed an antenna tuner resistive SWR test box shown in **Figure 1**. The resistors are Caddock 1% thick-film resistors with very good resistive properties well up into the VHF range. The 33 pF capacitor helps compensate for wiring inductance. The same SWR for both high and low impedances is provided in this test box; high impedance SWR cases present higher voltages, while low impedance SWR cases present higher currents.

A Simple Concept

The concept is simple. A fixed SWR is presented at the input to the box. The expected loss to an accurate power meter is easily determined. That is,

$$Loss = 10\log\left[(50 + R_{series})/50\right]$$

for the high-Z SWR case, or

$$Loss = 10\log\left[\frac{50}{50R_{shunt}/(50 + R_{shunt})}\right]$$

for the low-Z SWR case. Of course, the loss is the same for a given SWR regardless of whether it is a high-Z or low-Z case.

Figure 1 shows a schematic diagram of the resistive SWR test box. The parts list for the SWR test box is shown in **Table 1**. To that parts list you should add your choice of input/output connectors. I used an SO-239 connector for the input, since that is the interface used by most HF equipment.

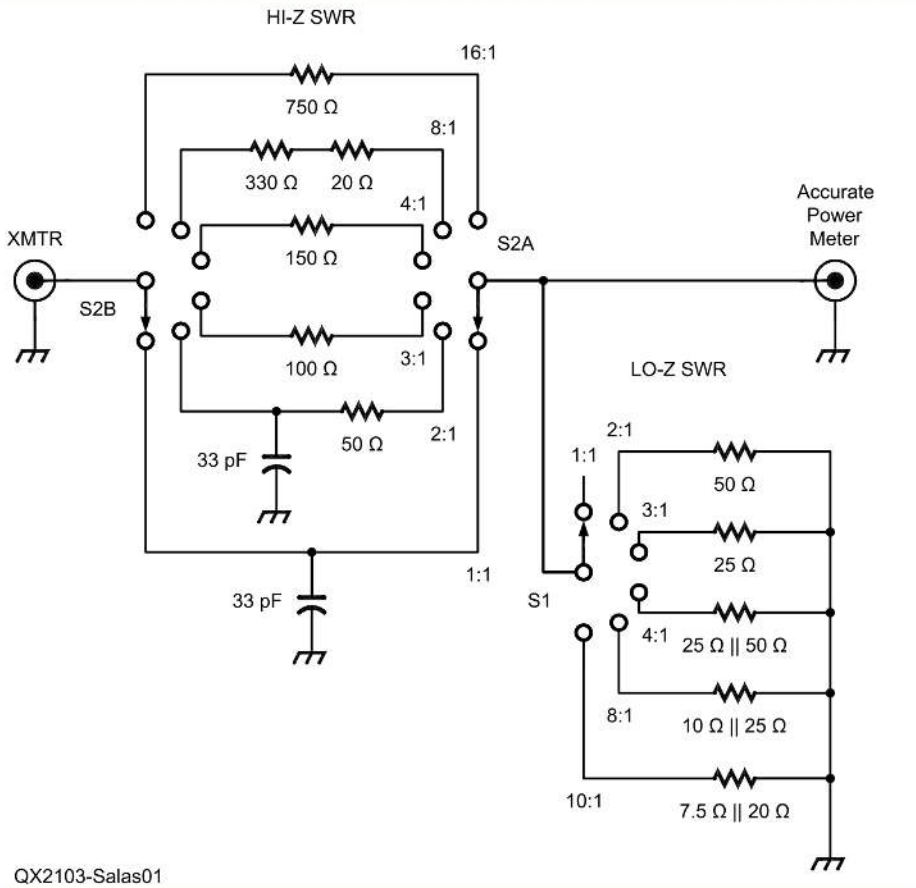

Figure 1 — Resistive SWR test box.

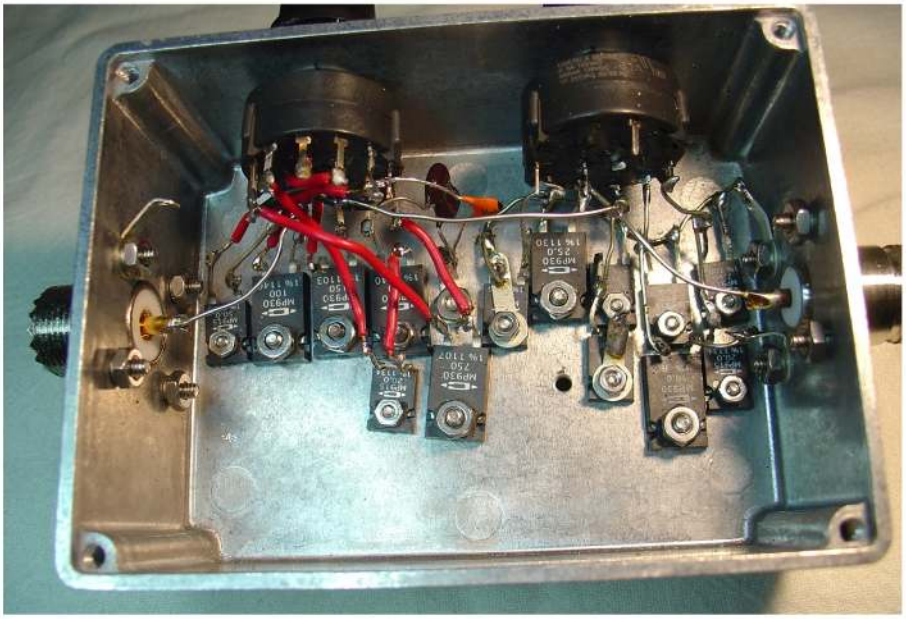

Figure 3 — SWR Test box internal wiring.

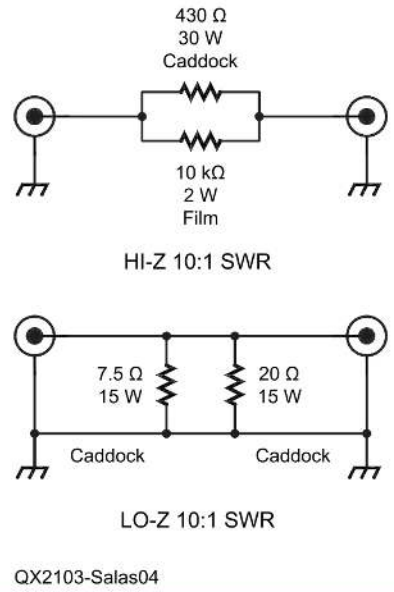

Figure 4 — Schematic of Hi/Lo fixture.

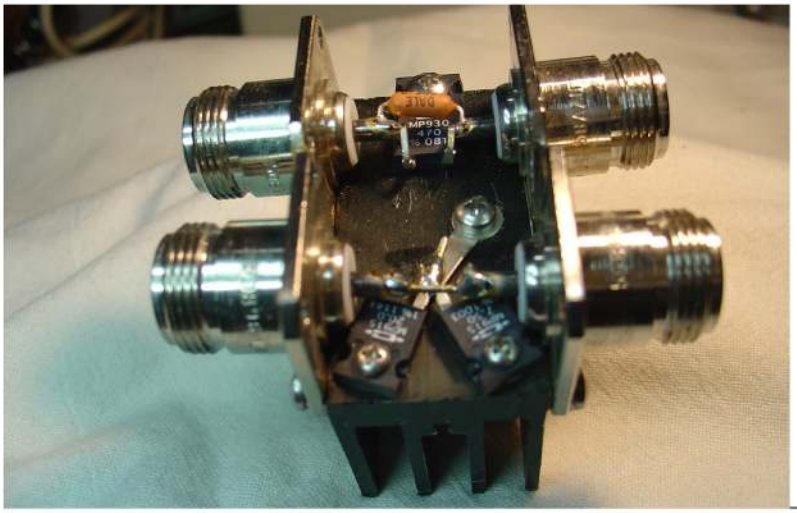

Figure 5 — 10:1 SWR Hi-Z/Lo-Z assembly.

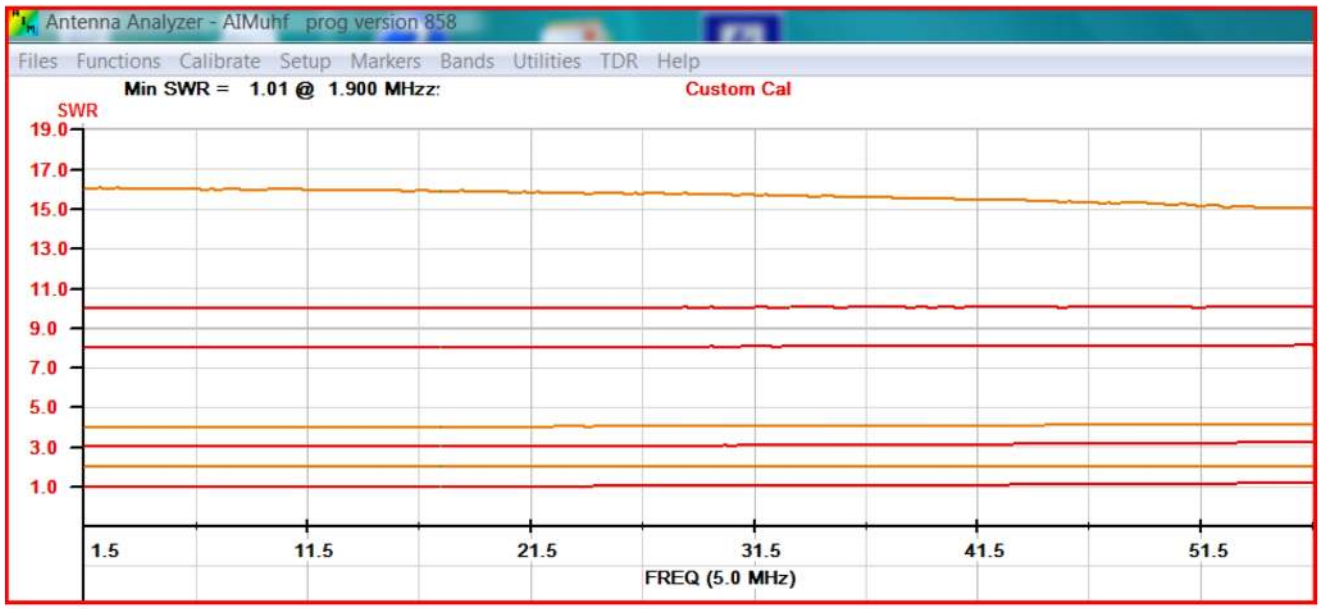

Figure 6 — High impedance SWR plots.

The output connector is type N, since this matches my attenuators and other test equipment. **Figure 2** is a picture of the front panel of the SWR test box, and **Figure 3** shows the internal wiring.

Because I didn't have a switch position for a high-*Z* 10:1 SWR section, I built a separate 10:1 SWR Hi/Lo fixture. While I didn't really need another low-*Z* 10:1 position, I went ahead and duplicated this since I usually make high-*Z* and low-*Z* readings of the same SWR sequentially. **Figures 4 and 5** show the schematic and completed assembly, respectively. **Table 2** is the parts list for this assembly.

Figures 6 and 7 show the high-*Z* and low-*Z* SWR plots of the SWR test box as measured with my Array Solutions AIMuhf analyzer. The 10:1 SWR high-*Z* reading was taken using the separate 10:1 SWR fixture of **Figures 4 and 5**.

Table 1
Parts list for the SWR test box of Figure 1.

QTY	*Description*	*Mouser Part Number*
1	2P6T Rotary Switch	PN 611-A20615KNZQ
1	1P6T Rotary Switch	PN 611-A10605RNZQ
1	750 Ω 30 W resistor	684-MP930-750
1	330 Ω 30 W resistor	684-MP930-330
2	20 Ω 15 W resistor	684-MP915-20
1	150 Ω 30 W resistor	684-MP930-150
1	100 Ω 30 W resistor	684-MP930-100
3	50 Ω 15 W resistor	684-MP915-50
1	25 Ω 30 W resistor	684-MP930-25
2	25 Ω 15 W resistor	684-MP915-25
1	10 Ω 30 W resistor	684-MP930-10
1	7.5 Ω 15 W resistor	684-MP915-7.5
1	AL Box	563-CU-5471
2	Knobs	450-2035-GRX

Figure 2 — SWR Test box front panel.

Table 2
Parts list for Hi/Lo 10:1 SWR test box of Figure 4.

QTY	*Description*	*Mouser Part Number*
1	470 Ω 30 W resistor Caddock resistor	684-MP930-470
1	10 kΩ 2 W resistor	71-CPF210K000FKE14
1	7.5 Ω 15 W Caddock resistor	684-MP915-7.5
1	20 Ω 15 W Caddock resistor	684-MP915-20
1	Scrap heat sink	
4	Connectors of choice	

Test Methodology

The test methodology is applicable to both manual tuners and auto-tuners. My reference test set-up is shown in **Figure 8**. Obviously you can use whatever test equipment you have as long as it is accurate. My Array Solutions Power Master and the MiniCircuits PWR-6GHS are NIST-certified and accurate to ±3%. The 6 dB high power attenuator helps keep the transceiver output stable, and provides an additional 12 dB of re-reflected power loss due to any less-than-ideal tuned antenna tuner input. Begin by verifying that the PowerMaster and MiniCircuits PWR-6GHS read the same (10 watts) with the SWR load box set to 1:1 SWR.

The actual measurement test set-up is shown in **Figure 9**. At each SWR measurement setting, after the antenna tuner has been tuned, set the transceiver output level so the PowerMaster reads exactly 10 watts. **Table 3** is the data table I use for recording the antenna tuner performance for each band tested.

Reactive Testing Load Box

Resistive matching tests are fine for antenna tuner comparisons. But it would be interesting to look at a few real-world impedance matching situations, especially when using remote antenna tuners. Remote tuners experience highest RF current and maximum inductance with short antennas. Higher-value matching inductance can mean higher loss due to the typically lower Q of a higher-value inductor. As an example, matching a 12 Ω resistive load on 80 meters requires an auto-tuner series-*L* of about 0.9 µH. However, a 43-foot vertical on 80 meters over perfect ground, which has a similar real resistance, has a high capacitive reactance as well ($13 - j\ 218$). For this antenna the series-*L* needs to be about 11 µH. So in order to determine auto-tuner losses in more real-world conditions, I built an antenna simulator circuit based on popular auto-tuner published minimum antenna length specifications. Because of its popularity, I also included a simulator for a 43-foot vertical on 80-meters.

Note that most auto-tuners — especially high power auto-tuners — do not have enough internal inductance to tune a 43-foot vertical on 160 meters. External inductance is usually required for 160 meter operation with 43-foot verticals.

Table 4 shows the *EZNEC* simulated impedances, and the actual circuit implementation components used. Excess

Table 3 – Antenna tuner loss data table.

Lo-Z SWR	*MC Lossless Power*	*Measured Power*	*Loss, dB*	*Loss %*
1:1	10 W (+40 dBm)			
2:1	5 W (+37 dBm)			
3:1	3.33 W (+35.2 dBm)			
4:1	2.5 W (+34 dBm)			
8:1	1.25 W (+31 dBm)			
10:1	1 W (+30 dBm)			
Hi-Z SWR	*MC Lossless Power*	*Measured Power*	*Loss, dB*	*Loss %*
1:1	10 W (+40 dBm)			
2:1	5 W (+37 dBm)			
3:1	3.33 W (+35.2 dBm)			
4:1	2.5 W (+34 dBm)			
8:1	1.25 W (+31 dBm)			
10:1	1 W (+30 dBm)			
16:1	0.625 W (+28 dBm)			

Table 4 – Impedances for antenna simulations.

Band	*Antenna Min. Length*	*EZNEC Ideal*	*Antenna Simulator*	*Antenna Simulator Measured*	*Simulator Reactance*
160 m	100 ft	18 – *j* 164	25 + 560 pF	24 + 580 pF	24 – *j* 152
160 m	90 ft	14 – *j* 222	25 + 390 pF	24 + 394 pF	24 – *j* 225
80 m	43 ft	13 – *j* 218	22.2 + 200 pF	21 + 211 pF	21 – *j* 215
80 m	33 ft	7 – *j* 344	16.7 + 130 pF	15 + 142 pF	15 – *j* 303
80 m	25 ft	4 – *j* 485	14.3 + 91 pF	13 + 100 pF	13 – *j* 430
40 m	8 ft	1.5 – *j* 643	16.7 + 36 pF	14 + 45 pF	14 – *j* 491

Figure 7 — Low impedance SWR plots.

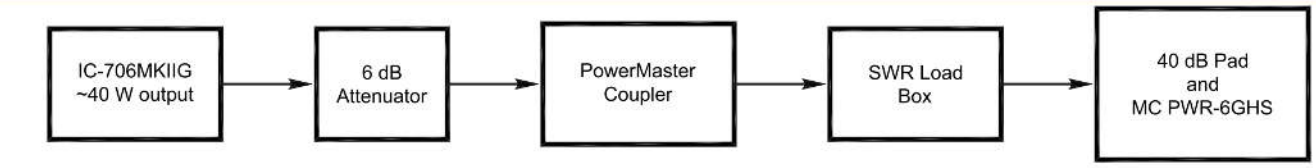

QX2103-Salas08

Figure 8 — Reference test set-up.

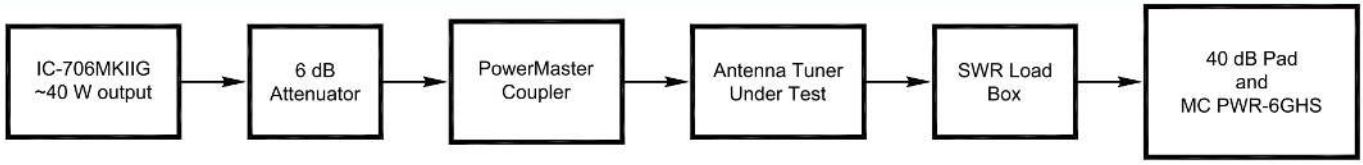

QX2103-Salas09

Figure 9 — Measurement test set-up.

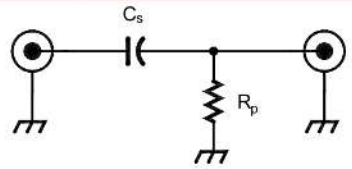

QX2103-Salas10

Figure 10 — Basic antenna simulator circuit.

Table 5 – Parts list for antenna simulator test box of Figure 10.

QTY	*Description*	*Mouser Part Number*
1	15 Ω 30 W resistor	684-MP930-15
1	20 Ω 30 W resistor	684-MP930-20
1	25 Ω 30 W resistor	684-MP930-25
1	40 Ω 30 W resistor	684-MP930-40
1	50 Ω 15 W resistor	684-MP915-50
1	560 pF 1 kV	598-CDV16FF561J03F
1	390 pF	598-CDV16FF391J03F
1	200 pF 1 kV	598-CDV16FF131J03F
1	130 pF 1 kV	598-CDV16FF131J03F
1	91 pF 1 kV	598-CDV18FF910J03F
1	36 pF 500 V	598-CD15ED360G03F
1	1P6T Rotary Switch	611-20725RNCQ
1	AL Box	563-CU-5471
2	Knobs	450-2035-GRX

Table 6 – Antenna Tuner Loss Measurements for Antenna Simulator Box.

Rp	*C Selected*	*Rp||50*	*Z tested*	*Power (ideal)*	*Power Meas.*	*Loss dB*	*Loss %*
15 Ω	36 pF	11.5 Ω	8 ft 40 m	2.3 W			
20 Ω	91 pF	14.3 Ω	25 ft 80 m	2.9 W			
25 Ω	130 pF	16.7 Ω	33 ft 80 m	3.3 W			
40 Ω	200 pF	22.2 Ω	43 ft 80 m	4.4 W			
50 Ω	390 pF	25 Ω	90 ft 160 m	5.0 W			
50 Ω	560 pF	25 Ω	100 ft 160 m	5.0 W			

Table 7 – Open/Short antenna tuner results.

Band	*Open Circuit*	*Short Circuit*
160 m		
80 m		
60 m		
40 m		
30 m		
20 m		
17 m		
15 m		
12 m		
10 m		
6 m		

Table 8 – SWR vs. Ham band for the SWR degradation box.

Band	*SWR*	*Fault forward power*
80 m	17:1	
40 m	5.6:1	
20 m	2.5:1	
17 m	2:1	
10 m	1.5:1	

resistance of about 5 to10 Ω was added to simulate real-world ground losses. The desired simulated antenna is selected by rotary switches.

The basic antenna simulator schematic is shown in **Figure 10**. Caddock thick-film resistors (*Rp*) are placed in parallel with a 50 Ω test measuring set-up to give the real resistance necessary. Series capacitors (*Cs*) simulate the reactive part of the hypothetical antenna and complete the physical simulation.

The different values of resistors and capacitors are selected by rotary switches in the completed assembly. The parts list for the antenna simulator box is given in **Table 5**.

Figures 11, 12 and 13 show the physical details of the antenna simulator box. **Figure 11** shows the internal view of the antenna modeling fixture. **Figure 12** is a top view showing simulator chart. **Figure 13** is a front view of the antenna simulator test box

The antenna simulation loss test set-up is shown in **Figure 14**. This is the same as the resistive load test set-up. **Table 6** is the data table that I use for determining the antenna tuner loss.

One final antenna tuner test is open/short testing, since this can also give an indication of antenna tuner loss. Ideally, the tuner should not be able to match an open or short circuit. However, many antenna tuners can on some bands, since they are able to tune into their own internal losses. In **Table 7**, hopefully all bands will show "No Match" when these tests are performed.

Conclusion

There is loss in every antenna tuner. With some extreme impedances, this loss can exceed 25%. So it is interesting and informative to be able to measure antenna tuner losses as part of a review process.

Addendum

While not related to antenna tuner loss measurements, I wanted to pass on a test box that I use to test SWR protection on solid-state amplifiers. My "SWR degradation" box consisting of a high-current 220 pF capacitor placed in series with a high power dummy load. This permits me to vary the SWR by simply changing bands. **Figures 15** shows an internal view of my SWR degradation box. **Figure 16** is an external view of the SWR degradation box.

For amplifier SWR protection tests, I start with low power and start increasing power into the test box on the different bands. Then I record the forward power at which a fault occurs on those bands. **Table 8** is the data table I use for listing the actual forward power versus SWR that causes the amplifier to fault.

Phil Salas, AD5X, an ARRL Life Member, has been licensed continuously since 1964. His interest in ham radio led him to pursue BSEE and MSEE degrees from Virginia Tech and Southern Methodist University respectively, followed by a 35 year career in RF, microwave and lightwave design. He held positions from design engineer to Vice President of Engineering. Now fully retired, Phil enjoys tinkering with ham radio projects and spending time with his two grandsons.

Figure 11 — Internal view of antenna modeling fixture.

Figure 12 — Top view showing simulator chart.

Figure 13 — Front view of the antenna simulator test box.

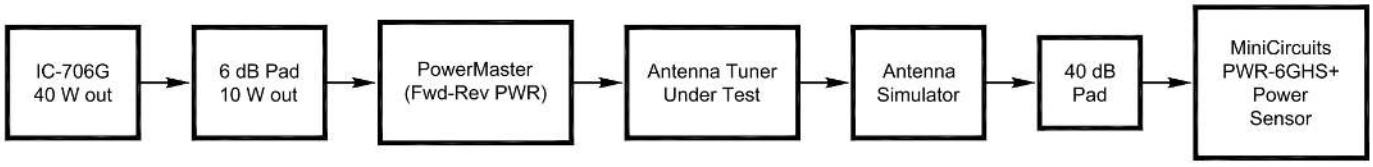

Figure 14 — Antenna tuner loss testing set-up.

Figure 15 — Internal view of the SWR degradation box.

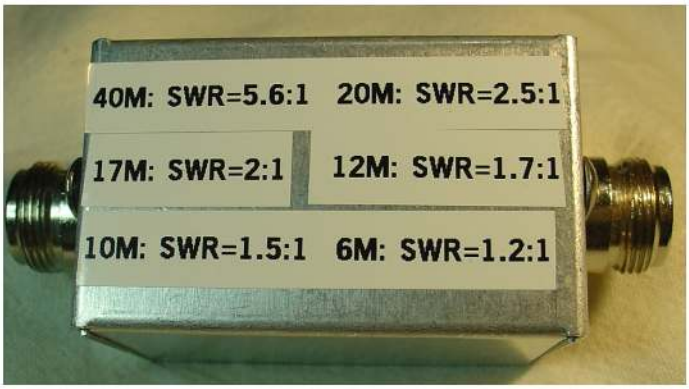

Figure 16 — External view of the SWR degradation box.

Hidetsugu Yagi and Shintaro Uda

both of Institute of Electrical Engineering, Tohoku Imperial University (1926)

Projector of the Sharpest Beam of Electric Waves

This reprint of the classic paper on the Yagi-Uda array has great historical significance.

Radio amateurs, and indeed commercial and government users, throughout the world make extensive use of the Yagi antenna — more accurately called the Yagi–Uda array. Hidetsugu Yagi and Shintaro Uda, two Japanese university professors, invented the Yagi in the 1920s. Uda did much of the developmental work while Yagi introduced the array to the world outside Japan through his writings in English.

Hidetsugu Yagi was born in Osaka, Japan, on January 28, 1886, and died January 19, 1976 in Tokyo, Japan. [Artwork by Christopher J. Dean, KD7CNJ].

Hidetsugu Yagi earned a graduate degree from the Tokyo Imperial University (now Tokyo University) in 1909. After four years of teaching at the Sendai Engineering High School, the Ministry of Education sent him on a European tour to further his education. He studied in Germany, working with Heinrich Barkhausen on generating CW oscillations by electric arcs, then in England where he worked with J. A. Fleming who invented the vacuum diode. He then came to the United States where he worked with George W. Pierce at Harvard University. Yagi returned to Japan and earned the doctorate from Tokyo Imperial University in 1921.

Shintaro Uda was a Japanese inventor and assistant professor to Hidetsugu Yagi at Tohoku Imperial University, where together they invented the Yagi–Uda antenna in 1926. Uda experimented with vacuum tube oscillators at wavelengths of 4.4 meter, and formed the waves into a directional beam using the antenna now known as the Yagi–Uda array.

Uda began antenna studies with experimental measurements on a single wire resonant loop. He improved the directivity by placing a below-resonance parasitic loop near the driven loop. That evolved into parasitic rods. He found that placing more rods resulted in higher directivity. Uda found that greatest directivity occurred when reflector rods — about 10% longer than a half wave in length — were placed slightly more than a quarter wave from the driven element, and director rods — about 10% shorter than a half wave — were spaced slightly more than a third of a wavelength.

Shintaro Uda was born in Nyuzen, Toyama, Japan on June 1, 1896, and died August 18, 1976. [Artwork by Christopher J. Dean, KD7CNJ].

In February 1926, Yagi and Uda published their report on the wave projector antenna, reprinted here with permission from the *Proceedings of the Imperial Academy (of Japan)*, Volume 2 (1926) Issue 2, pp. 49-52.

18. *Projector of the Sharpest Beam of Electric Waves.*

By Hidetsugu YAGI and Shintaro UDA.

Institute of Electrical Engineering, Tohoku Imperial University, Sendai.

(Rec. Jan. 9, 1926. Comm. by Hantaro NAGAOKA, M.I.A., Jan. 12, 1926.)

Suppose that a vertical antenna is sending out electro magnetic wave in all directions around it. If a straight metallic rod of finite length be vertically erected within the field of its propagation, then the behavior of this metal rod will be as follows :—

When the length of this rod is equal to or slightly longer than a half wave length, the current induced in it will be in phase with or lagging behind the E.M.F. caused by the electric wave, and the rod will act as a " Wave reflector."

If, on the other hand, the length be made somewhat less than a half wave length, the current induced in it will be leading before the E. M. F., and the rod will act as a " Wave director ".

A single wave reflector placed behind a radiating antenna is sufficient to cause directive radiation of radio wave. It is especially efficient when placed a quarter wave length behind the radiating antenna. Again a wave director placed in front of and more than a quarter wave length distant from the radiating antenna is also effective in producing a directive radio wave.

When several wave director rods are arranged along a line with intervals equal to or more than a quarter wave length, the wave energy will be projected chiefly along this line, and the series of these wave directors forms what the authors will call a " Wave duct " or a " Wave canal ' .

According to the authors' experience, a parabolic reflector is not necessary for producing a beam of radio wave. The simplest and comparatively effective reflector may be formed as stated below.

A wave reflector rod is placed a quarter wave behind the antenna and two more wave reflectors, one being on the left and the other on the right side of it, are placed a half wave distant from the antenna. (Fig. 1.) These three rods form a tri-antennary reflecting system which will hereafter be called a fundamental " Trigonal reflector ".

Fig. 1.

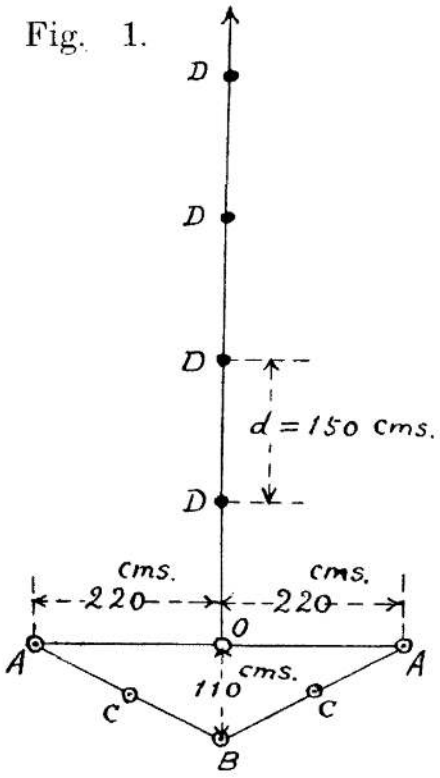

Wave length $\lambda = 400$ cs.
0 .....Sending or receiving antenna
A.....Side reflectors
B.....Back reflector
C.....Screening reflectors
D.....Wave directors
◉.....Brass rod, 220 cms. long
●.....Brass rod, 180 cms. long

Fig. 2.

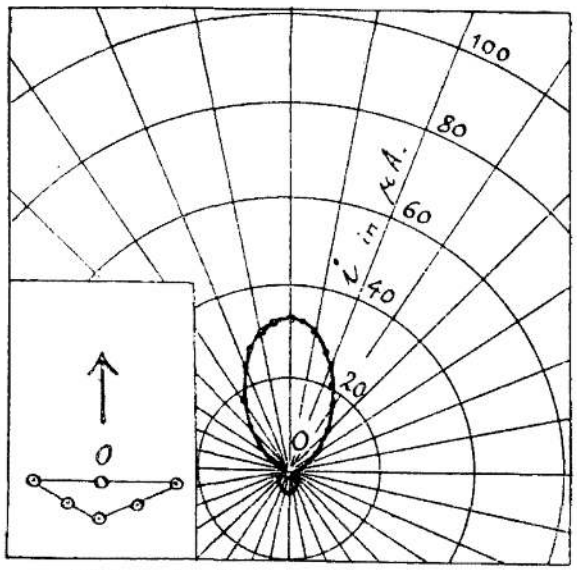

Trigonal reflector with 5 rods.
Wave length = 440 cms.
Length of reflector rod = 220 cms.

Two more reflector rods C C are shown in Fig. 1. These are not as efficient as a reflector as A and B's, but their existence enables closer screening of waves in the backward direction, and when this reflector system is employed in a receiving station, they are specially effective to eliminate external disturbances from behind.

Combined with these screening rods, the trigonal reflector is now formed of five rods. The position of the screening rods are nearly midway between A nd B, and a slight variation of their position is practically ineffectual.

When the trigonal reflector is employed in a receiving station, it may better be called a " Trigonal collector ".

Now the projection of the sharpest beam ever produced of electric waves can be effected by the combination of a trigonal reflector and a wave duct. This combination will thus be called a "Wave projector." It is also very advantageous to employ a wave duct and a trigonal collector at receiving stations.

The directivity can be improved by increasing the number of wave director rods contained in the wave duct. As an extreme case, when the sending and the receiving stations are connected with a line of wave canal, the transmission of wave energy can be the most efficaciously accomplished.

Some typical results of observation with short electric wave are given below. Fig. 1. shows the plan view of the arrangement of conductors for the wave length

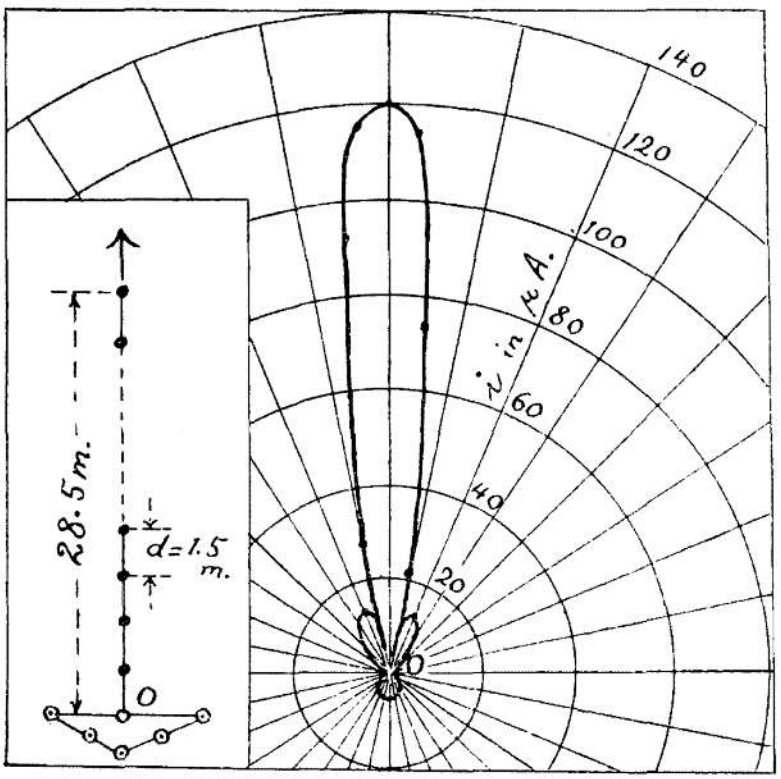

Fig. 3.

Wave projector.

Wave length = 400 cms.

◉ 5 rods, 220 cms. long

● 19 rods, 180 cms, long

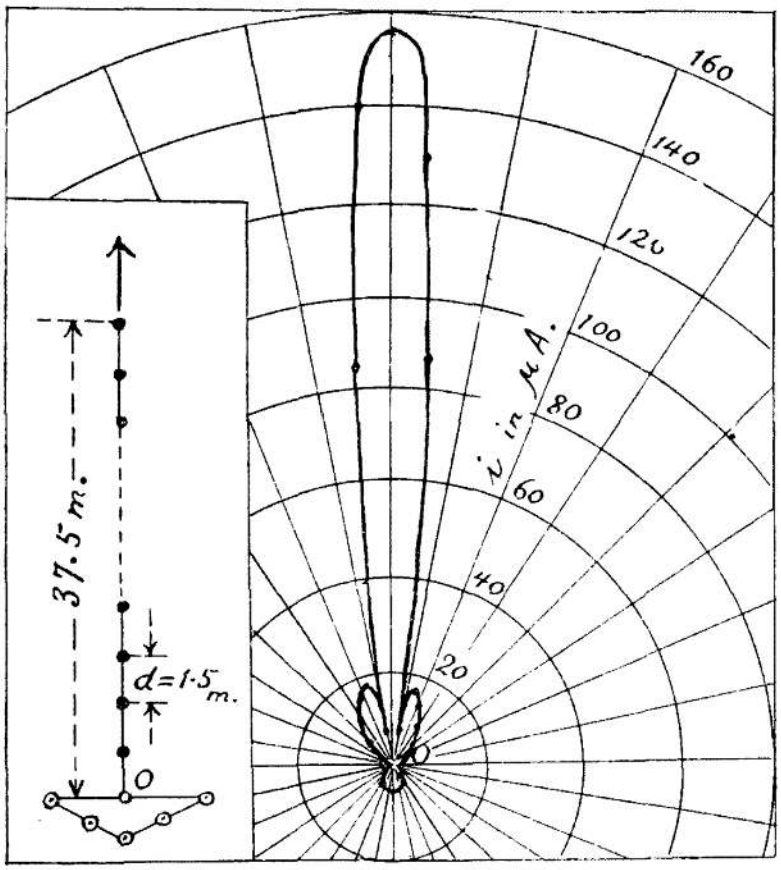

Fig. 4.

Wave projector.

Wave length = 400 cms.

◉ 5 rods, 220 cms. long

● 24 rods, 180 cms. long

of 4.4 metres.

In Fig. 2. is shown the directive effect of a trigonal reflector with five rods. No wave director is here employed, and the intensity is measured with a receiving system comprising a crystal detector and a galvanometer. It has been very carefully ascertained that this crystal system gives tde most consistent results throughout the long time of experiments.

In Figs. 2. 3. and 4., the radius vector of the polar diagram gives the measure of intensity in the receiving system placed in that direction, the distance from the sending station being kept constant.

Now if the wave duct or wave canal is provided, the directivity becomes remarkably augmented. In the case of Fig. 3., 19 rods of 180 cms. length (a half wave being equal to 220 cms.) were arranged along a line with interval of 150 cms. (a quarter wave being equal to 110 cms.). In the case of Fig. 4., 25 rods of 180 cms. length were set up with interval of 150 cms. The length of all the reflector rods was made equal to the half wave length, i.e. 200 cms.

The field measurements were made under the same conditions, and the short wave generator was also kept at exactly the same condition for all the observations of Fig. 2., Fig. 3. and Fig. 4.

It is easy to explain how the radiation in the side direction becomes minimum, and the polar diagrams prove the realization of the sharpest beam ever produced of electric waves.

Many observations of various cases have been made in the Tohoku Imperial University, Sendai, and further details will in time be published in the Journal of the Institute of Electrical Engineers of Japan.

Robert J. Zavrel, W7SX

P.O. Box 28756, Spokane, WA 99228; **w7sx@arrl.net**

A Four-Band Two-Element W7SX (Zavrel) Array

This center-fed two-element array achieves improved gain by using a new parasitic element design.

This article describes a two-element W7SX array for 4 bands — 40, 30, 20, and 17 meters. [The W7SX or Zavrel array differs from a conventional Yagi array in that the element lengths are not restricted to around a half wavelength. — *Ed.*]. **Table 1** shows a gain comparison of the W7SX array with the a equivalent gain of full-size Yagi-Uda arrays.

Table 1 – Gain comparison of a multiband W7SX array with equivalent monoband Yagi array.

Band	*W7SX element length*	*equivalent Yagi elements*
40 m	0.50 wavelengths	2
30 m	0.75 wavelengths	2
20 m	1.00 wavelengths	3
17 m	1.25 wavelengths	3

I introduced this new technique in the January/February 2017 issue of *QEX*. In the May/June 2017 issue under *Letters*, Randy Rhea, N4HI, called it the "W7SX array!" In my ARRL book *Antenna Physics, an Introduction*, I described a relatively little known, among radio amateurs, characteristic of antenna elements called the "scattering aperture." This "scattering" of radiated RF power is what makes parasitic elements possible, and can result in substantially higher gain from a given array than phased driven elements. This is what makes the Yagi and W7SX configurations such effective antennas.

Since its inception [see "Projector of the Sharpest Beam of Electric Waves," by Hidetsugu Yagi and Shintaro Uda (1926), reprinted elsewhere in this issue. — *Ed.*], Yagi designs have concentrated on making all the element lengths close to ½ wavelength with the driven element at resonance, the reflector a bit longer and the director(s) a bit shorter. Only a small deviation from the resonant length causes the phase of re-radiated (scattered) power to create reinforcement and/or cancellation of power in the desired directions. This creates the unidirectional directivity of the Yagi array.

There is no reason to limit the length of a parasitic element to near ½ wavelength resonance, other than being able to feed the driven element directly with coaxial line. However, in most cases *some form* of matching is needed along with a balun function since the driven element is balanced and the feed impedance is usually lower than the 50 Ω feeder. With the introduction of computer-controlled automatic tuning equipment, an open-wire feeder could feed such a tuning device at the base of the tower. Such a tuner could be custom designed for the bands covered by the antenna, with fixed elements achieving a basic tuning and then perfect tuning accomplished by an auto tuner. This would permit a perfect match at the antenna for a single 50 Ω lead. Therefore the tuner could be specially designed for a given multi-band array.

In multi-band Yagi designs, much of the length of elements is "wasted" by the mantra of limiting the electrical lengths to near ½ wavelength on the higher frequencies by using traps and/or a variety or techniques to limit the electrical length to the precious ½ wavelength. The possible effective lengths for straight, unloaded elements to be used effectively ranges from a bit shorter than ½ wavelength to 1 ¼ wavelengths, the length of an extended double Zepp. The W7SX antenna described here uses a conventional Yagi design for 40 meters (the elements are close to ½ wavelength long); on 30 meters the elements are about ¾ wavelength long; on 20 meters elements are about 1 wavelength long (2 element collinear, with a 2-element collinear reflector); and on 17 meters elements are 1 ¼ wavelength long (extended double Zepp).

Any element length in this range can be made into a parasitic element by placing an appropriate reactance at the center of the element. For example, it is a well-known technique to place an inductor at the center of an element shorter than ½ wavelength to create a director or reflector. Little known among Yagi designers is that if the element is too long it can also be configured as a parasitic element. It is well known that increasing an element length more than ½

wavelength, the broadside gain increases until the maximum is reached at 1 ¼ wavelength (the double extended Zepp) where the gain is about 3 dB higher (3 dBd) than the standard ½ wave dipole. This starting point is a great advantage, since the maximum gain from a full size 2-element Yagi is about 5 dBd. Consequently the maximum gain from a 2-element W7SX antenna using 1 ¼ wavelength elements is about 8 dBd, which is close to the gain of a standard 4-element Yagi!

Figure 1 shows the approximate reactances needed to create a parasitic element from elements that are ½ to 1 ¼ wavelengths long and also plots the increase in gain for an increase in element lengths. This is for a 2-element antenna with the driven and reflector elements fixed at 1/8 wave spacing. The element lengths are the free space fractions of a wavelength.

In **Figure 1** we see that by using the exact length of slightly longer than ½ wave, no reactance is needed. As the element is made longer, a reactive value is needed to create the optimum parasitic configuration. The element separation also affects this parasitic value, so 1/8 wavelength separation is used for this data. Also, the driven element uses the same length as the reflector.

Figure 2 shows a picture of the array. The driven element is fed with home brew open wire line that runs to the shack about 500 feet down the mountain. The antenna is located at the peak and all anchors are mounted in the granite outcroppings, including the guy anchors and tower base.

Figure 3 shows the electrical box attached to the 3" boom and holds the reactive components and relays. Two bare copper wires run from the bottom of the box to the 3" diameter element sections. A wire for the relay controls is shown in the upper left corner attached to the boom. When the tilt-over antenna is up the lid of the box faces downward, hence the drain holes in the top.

Figure 4 shows an *EZNEC* picture of the array. The driven element is simply fed directly with open wire transmission line. All adjustments for the reflection (in effect the band switching) are performed in a single box mounted at the center of the reflector.

Design Methodology

If we want to create a multi-band antenna from a single-band Yagi, the first step can be very simple if the bands of interest are harmonically related. This simple idea drove the author to first create a 40/20 meter W7SX array. The two sides of the reflector's center are simply shorted for 40 meter operation creating a simple 2-element Yagi. On 20 meters, the center is opened to create two co-liner ½ wave reflectors. The driven element also becomes a 2-element collinear configuration. This results in a 4-element collinear W7SX array. The equivalent gain is comparable to a full size 3-element Yagi, since the spacing between the elements in a collinear array is very small. If the reflector element lengths are set for maximum gain on 20 meters, the length for 40 meters (when shorted) is slightly short for best performance when using a relay. I simply place a 1 to 2 µH inductor across the gap and achieve near-optimum performance on both bands.

Here I show three methods of switching between 40 and 20 meters. **Figure 5** illustrates the first method for band switching, a simple DPDT switch. On 20 meters it opens the center and on 40 shorts the center through a small value inductor. This could also be a DPST switch.

Shown in **Figure 6**, the second method uses an open wire line with an electrical length of ½ wavelength on 20 meters with the end left open. This results in an open condition at the reflector's center and a short on 40 meters. This simple technique

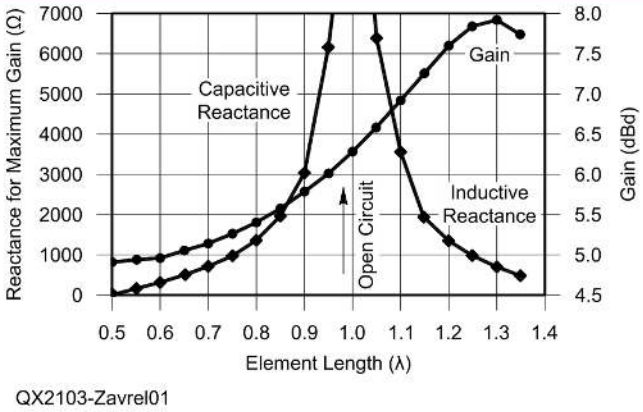

Figure 1 — Reactances needed to make a parasitic element from elements ½ to 1 ¼ wavelengths long , and the increase in gain for an increase in element lengths.

Figure 2 — The W7SX array. The open-wire transmission line is seen on the right.

Figure 3 — An electrical box attached to the 3" boom houses the reactive components and relays.

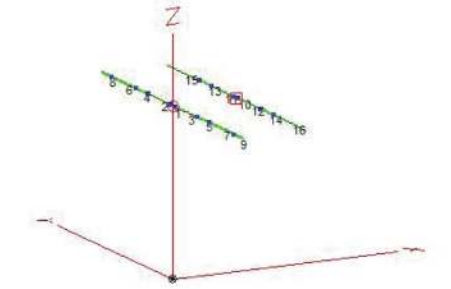

Figure 4 — An *EZNEC* rendering of the W7SX array.

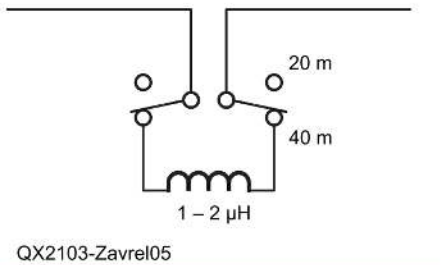

Figure 5 — One method for band switching uses a DPDT switch.

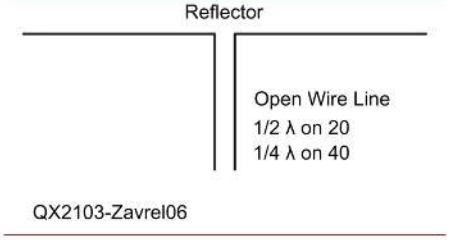

Figure 6 — Another band switching method uses an open wire line stub.

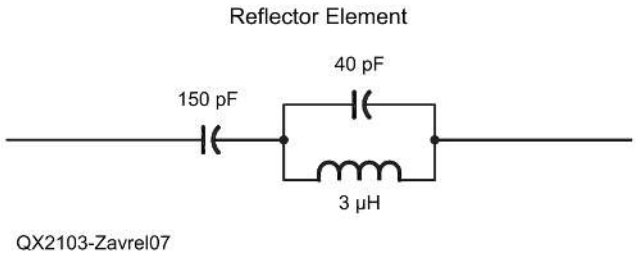

Figure 7 — Another band switching method uses a 20 meter trap in the element center.

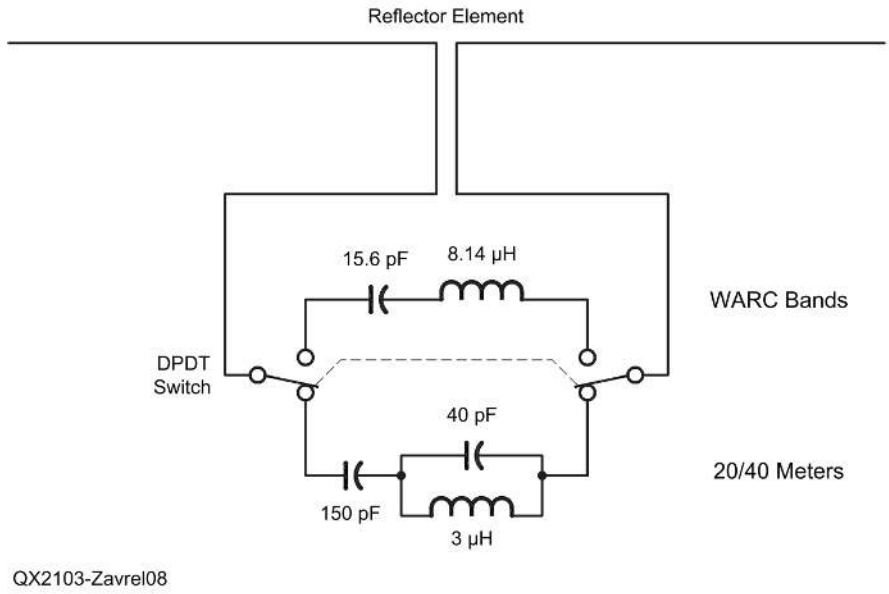

Figure 8 — This configuration uses a single DPDT switch (relay) that selects 20/40 meters or 30/17 meters.

provides for "automatic" band changing.

Figure 7 shows that a third way to break the reflector at the center is to use a 20 meter trap. However, this also creates too much inductance at the center on 40 meters. This can be tuned out with a capacitor adjusted to just the right amount of reactance on 40. Use standard equations for the reactance of a parallel *LC* tank and then use an appropriate capacitance to "tune" the reactance to a desired value.

On both 30 and 17 meters, the reflector is considerably off resonance. **Figure 1** is presented to show the basic relationships between the length of the reflector and the necessary reactance to form an effective reflector. For detailed designs, it is best to model the antenna for specific dimensions and then empirically determine the best reactive value(s). There will be a small variation to optimize the element for maximum forward gain or maximum front-to-back ratio similar to the common practice of fine adjustment of the length of the reflector.

On my array I used *EZNEC* modeling to derive the optimum capacitor and inductor values for 30 and 17 meters. It is also possible to place a reactive value on the physical antenna and simply tune for maximum gain. This is simple for a capacitor requirement, you simply use a variable capacitor, tune for maximum gain and then measure the capacitance at the tune point. To create a variable inductor, you can simply use an inductor in series with a variable capacitor, then measure the equivalent inductance across the *LC* series circuit after tuning for maximum gain. Once you know the desired values, you can install fixed components.

I gained confidence in the *EZNEC* model, thus I used *EZNEC* to determine the necessary capacitive and inductive values for 10.1 and 18.1 MHz. For 30 and 17 meters they are –492 Ω and +364 Ω respectively or translated into component values, 32 pF and 3.9 µH.

Now, if we construct the proper *series LC* circuit we can provide the proper reactances

for both 10.1 and 18.1 MHz without needing to switch between the two. The calculation can be accomplished using a set of two simultaneous equations that directly solve for the needed X values of the series circuit for the desired frequencies. Simultaneous equations can get rather nasty when you have multiple variables. However, you can use a much simpler set of two equations. Fortunately, the ratios for reactances remain *constant* between two fixed frequencies. For example, a fixed capacitor with have 0.558 of the reactive value at 18.1 than it has at 10.1 MHz. It will also have 1.792 the value of inductive reactance for a fixed inductor than at 10.1 MHz. The ratios are simply 18.1/10.1 and 10.1/18.1.

Armed with these ratios, we can construct two equations,

$$1.792X_L - 0.558X_C = +364\ \Omega \text{ (for 18.1 MHz)}$$
$$X_L - X_C = -492\ \Omega \text{ (for 10.1 MHz).}$$

When you solve the equations the final results are derived from the 10.1 MHz reactive values. You then calculate the actual L and C values from these values, and you're finished. You have the values to use in the series LC circuit. The answers are,

$X_L = 517\ \Omega$ or 8.14 µH,

$$\text{where } L = \frac{517}{2\pi\, 10.1\text{ MHz}}$$

$X_C = 1009\ \Omega$ or 15.6 pF,

$$\text{where } C = \frac{1}{(1009)2\pi\, 10.1\text{ MHz}}.$$

For those who do not know how to solve simultaneous equations for two variables, there are multiple sites on the internet that allow you to easily solve them. The simplified form of these equation makes using these calculator sites very easy.

NOTE: Similar to almost any antenna design, the exact C and L values may be a bit different than the modeled values. In this case, for maximum performance, you can check for maximum gain (or maximum F/B ratios) by adjusting the C or L on each band. Then calculate the revised reactive values and use those values in the equations. However, the modeled values will most likely be fairly close to optimized values for a given antenna design, tower, height, and the usual variables for a given site.

Figure 8 shows a configuration using just one DPDT relay to select 20/40 meters or 30/17 meters. In my case I use two relays, one for the WARC series LC network and the other for an open for 20 m and a small inductor for 40 m. This allows me to disengage the reflector on 40 or 20 m for testing gain (in dBd) and/or being able to copy off the back of the array.

Table 2 – W7SX array performance in free space.

Frequency, MHz	*Max gain, dBd*	*F/B, dB*	*Beamwidth*
7.1	4.78	5.81	64.4°
10.1	4.87	6.36	58.4°
14.1	5.53	6.83	45.8°
18.1	6.75	4.75	28.6°

W7SX Array Performance

The response on the four bands for this antenna is summarized in **Table 2**. The data were computed in free space at 0° elevation angle. The dBd gain is referenced to a ½ wave dipole. For dBi simply add 2.15 dB. This W7SX array antenna was designed for maximum forward gain; better front-to-back ratio designs are also possible.

Bob Zavrel, W7SX, was first licensed in 1966. He has worked in RF engineering for his entire career working primarily in RF semiconductors and antennas. He published the first block diagram of an SDR system in 1987, invented the 8-circle antenna array, has published over 100 papers and articles in both professional and amateur publications, and has 7 patents. He has achieved DXCC Honor roll (mixed and CW) and 5BWAZ (200) using only tree supported wire antennas. He is currently an RF business and technical consultant, a volunteer technical advisor to the ARRL, ARRL Life Member, adjunct engineering professor at Gonzaga University, author of the ARRL publication Antenna Physics, an Introduction, and Senior Member of the IEEE. Bob has an BS in Physics from the University of Oregon.

Errata

• In Steve Stearns, K6OIK, "*HOBBIES* Software for Computational Electromagnetics," *QEX* Nov./Dec. 2020, "frustums" is misspelled in **Figure 1**. In **[3]**, the name "M. B. Dragović" is misspelled. The correct citation is, B.D. Popović, M.B. Dragović, and A.R. Djordjević, *Analysis and Synthesis of Wire Antennas*, Wiley, 1982. The following new instructions apply.

Purchase the book, Y. Zhang, et al., *Higher Order Basis Based Integral Equation Solver [HOBBIES]*, John Wiley & Sons, 2012. Download and install *HOBBIES* academic version 10.5.1 from **https://www.hobbies-em.com**. Then contact *HOBBIES* support, **support@hobbies-em.com**, to request a license. Tell *HOBBIES* support that you don't have a registration key because Wiley does not supply it or a CD-ROM with the book anymore. They may ask for proof of book purchase. You can also request a 30-day free trial of *HOBBIES* professional from *HOBBIES* support.

A *HOBBIES* software license incorporates a GiD license. GiD, developed by CIMNE in Spain, performs pre-processing geometry editing and meshing, and post-processing graphics. *HOBBIES* uses GiD version 9. You can download the GiD version 9 manual from **https://www.gidhome.com/support/gid-manuals/manuals-archive**.

A *HOBBIES* license file is locked to a particular disk, so to make *HOBBIES* totally portable, use a USB drive for everything (license files, the downloaded zip installation files, and your .gid project folders). You can then use any Windows x64 computer by inserting the USB drive and running *HOBBIES*. Remember to backup all files including the hidden license files that are on the USB drive.

HOBBIES can run in serial or parallel mode, using either in-memory or out-of-memory solvers. You can use parallelization to speed up calculations as described in chapter 4 of Zhang and T.K. Sarkar, *Parallel Solution of Integral Equation-Based EM Problems in the Frequency Domain*, John Wiley& Sons and IEEE Press, 2009.

• In Eric Nichols, KL7AJ, "Derive Everything" Sidebar of "Self-Paced Essays – #3 EE Math the Easy Way," page 21, Jan./Feb. 2021 *QEX*, the last incomplete sentence should be, "We can substitute basic "ingredients" from well-known, fundamental equations, and create new derived formulas more suitable for our immediate purposes." Thanks to Glen W. Ruch, KA9VCA, for spotting the omission.

Jerry Spring, VE6TL
206 Hampstead Place NW, Calgary, AB, Canada T3A 5J2; jspring@telus.net

The Onset of Solar Cycle 25 and the MG II Index

The MG II index may have already indicated the transition between Cycle 24 and Cycle 25.

Introduction

In March of 2020, I began noticing slight improvements in shortwave radio (HF) propagation from my station in Alberta, Canada. The solar indices revealed little change as the solar flux index (SFI) remained around the 70 mark and the Sunspot number had been at zero for many consecutive days. Even the solar wind remained well below its "normal" 400 km/s, as there were few coronal holes to encourage it. So was I imagining things? Or was there some other measurement, beyond those commonly published on solar weather websites that could explain significant improvements in shortwave propagation?

Further research suggested that the answer may be found in extreme ultraviolet (EUV) radiation and its interaction with the topside layer of Earth's ionosphere during the solar minimum. Scientists have been studying this phenomenon for many years, specifically as it relates to climate change. Yet, changes in solar irradiance, the power per unit area emitted by the Sun in the form of electromagnetic radiation, not only has a profound impact on the Earth's climate, but the same measurements can yield useful information about subtle fluctuations governing the ability of the ionosphere to refract radio waves. It is proposed here that a more useful and reliable proxy relating to amateur radio HF DXing during solar minimum measure can be found in a specific band of energy emitted by magnesium ions from within the Sun. This is referred to as the MG II index, calculated from a pair of spectral lines (doublet) at a wavelength of approximately 280 nm **[1]**. The good news is that while climatologists and geophysicists are using this index for their studies, amateur radio operators can also take advantage of the daily published index **[2]** and thereby create a more accurate prediction of HF radio wave propagation. It is the aim of this paper to familiarize the amateur radio community with the MG II index while also suggesting its utility during solar minimum, where it may have already indicated the transition between Cycle 24 and Cycle 25. This is still a work in progress, but like most DXers, it would be nice to see a more active Sun.

1 – Sunspots and the Solar Flux Index

Many DXers and contesters are already familiar with a number of solar indices. Two of the most commonly used are the Sunspot number (Rz) and the SFI. During the past two solar minima, the Sun has averaged nearly 800 spot-free days in each cycle, yet solar weather during these times has varied considerably. Thus, Sunspot-based predictions of HF propagation are not very helpful over large portions of the 11 year cycle. The SFI, on the other hand, correlates well with sunspots, solar flares, and CMEs (coronal mass ejections), and has proven to be a fairly reliable indicator of solar weather during the more active parts of the cycle. In order to measure the solar flux, ground-based daily measurements of incoming solar radiation intensity at a frequency of 2800 MHz (10.7 cm wavelength) are made using a solar radio telescope. Since daily measurements began in 1947, the SFI varies from about 65 to 450 $Wm^{-2}Hz^{-1}$. Yet during solar minimum, a one to two year period where the Sun's output is lowest over an 11 year cycle, the values of the SFI tend to remain in a narrow range, typically 67 to 72, and frequently fail to predict improved "DX windows." From discussions with other radio operators over the years, the conventional wisdom is that there is no substitute for listening to the bands, rather than relying solely upon solar indices or other measurements. Yet, with the MGII index, perhaps this too can change.

During the solar minimum, many of the measurements or indices commonly posted on solar weather websites are of little help in forecasting HF propagation. This is because the majority of these measurements react to solar storms, which generate increased activity in X-rays, proton flux, electron flux, magnetic flux, etc. Yet, during spotless times, I have continued to observe solar activity in the form of brighter spots as seen only in the EUV portion of the EM spectrum (defined as the range from 10 to 120 nm) thanks to NASA's Solar Dynamic Observatory (SDO) **[3]**. This satellite was launched in 2010 and has been continuously providing valuable solar weather information until the present day. Thanks to a number of different instruments, it provides views of the Sun's

irradiance at many different wavelengths, from the visible continuum to the extreme ultraviolet.

The images in **Figure 1** were taken on May 18, 2020 and show the Sun's visible continuum, as well as the irradiance at a wavelength of 131 nm — in the near EUV portion of the spectrum. In the absence of sunspots at visual wavelengths, two bright areas (referred to as "plage" events) stood out. The word *plage* comes from the French, meaning *beach* as these are bright spots — as opposed to dark sunspots — which resemble a bright beach. They are caused by thin tubules of magnetic flux within the chromosphere of the Sun and represent regions of significantly higher temperature than their surroundings. Sunspots, by contrast, represent cooler regions of the Sun. Both phenomena are created by the intersections of magnetic flux lines in complex ways.

While reviewing the **Figure 1** images, several reports arrived via social media where amateur radio operators within North America were experiencing 10 m openings, presumably not just sporadic-E. There were also openings on 15 m and 20 m that were better than they had experienced in many months. These reports were confirmed by reviewing online sources such as *PSK Reporter* **[4]** and *DX Maps* **[5]**. With the SFI at 69, the planetary A and K indices extremely low (no magnetic storms) and the solar wind "normal" (below 400 km/sec), it appeared that a key measurement or index associated with the EUV plage events was lacking – one that could relate anomalies in the EUV images to the anomalous propagation. This prompted a more rigorous investigation in search of such an index.

Combing through a number of technical papers, it became clear why many of the common measurements or indices failed to yield accurate predictions of HF propagation during solar minima. One paper stated, "Statistical analysis showed that both the Sunspot number and SFI follow the amplitude of solar EUV in a nonlinear way. Moreover, the solar proxies and EUV are not well correlated on short-term scales (*e.g.* the day-to-day variation) mainly because solar radiation at different wavelengths originates from different sources" **[6]**. The main issue with the solar flux index is that it is measured from the ground, which sees only the "bottomside" of the ionosphere. Yet, solar EUV radiation is almost entirely absorbed before entering the lower atmosphere, which means space-based measurements are required in order to study the "topside" of the ionosphere where critical ionization reactions are happening — especially during the solar minimum.

Another problem with the SFI measurement is that during a solar minimum, it fails to reflect low-level variations in solar irradiance. Many hams (including me) have commented that the index appears "stuck" around 69 or 70 for long periods of time. This is because "the quiet Sun component produced by Bremsstrahlung emission over the entire Sun dominates the observed emission, as any remaining active regions are no longer strong enough to produce additional radio emission" **[7]**. In other words, minor changes in solar irradiance during the solar minimum are frequently beyond the resolution of the SFI measurement.

A third issue with SFI is that it assumes a uniform ionospheric chemistry throughout the 11 year solar cycle. Yet, it has been shown that the composition and density distribution (scale height) of various ions change throughout the cycle. For example, the topside layer is dominated by H+ ions during the solar minimum and by O+ ions during the solar maximum **[8]**. This suggests the effects of EUV radiation on the topside of the ionosphere change with time. Again, the only really effective means of determining the influence of small changes of EUV irradiance on the topmost layer of the ionosphere is via space-based measurement. At the higher frequencies in the HF radio spectrum (10 m and 6 m), it is the topmost layer of the ionosphere that figures most prominently in refracting these waves back towards Earth. It therefore becomes highly desirable to have a physical measurement that serves as a proxy for ionization activity in this layer. The MG II index serves this function.

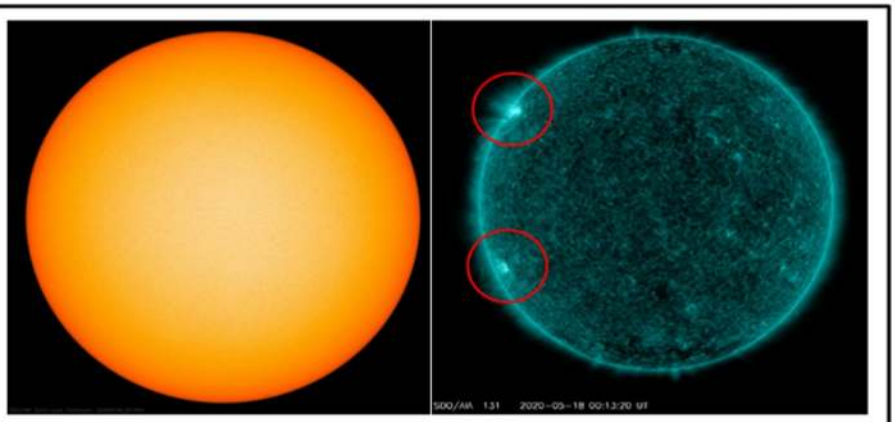

Courtesy NASA

Figure 1 — Solar visual continuum *vs.* EUV at 131 nm.

2 – The MG II Index

Every element in the periodic table exhibits a unique "fingerprint" when its electrons are sufficiently excited by external forces. The transition from one energy state to a lower one results in the emission of electromagnetic radiation (photons) at different wavelengths. By passing the EM radiation through a spectrograph or spectrometer, the unique wavelengths can be measured and the element identified. Moreover, the strength or intensity of these lines is related to the amount of energy present, which can be correlated to the exciting forces (coming from within the Sun). With many different elements to choose from in the Sun it was discovered that magnesium ions emit particularly useful spectral lines. At a wavelength of 280 nm (considered within the UV band of wavelengths), a pair of closely spaced, bright spectral lines are observed, known as a "doublet." This doublet provides one of the most highly variable and yet dependable proxies for solar irradiance. The doublet "signature" and its neighboring wavelengths comprise what is referred to as the MG II index **[9]**. This index offers several advantages over other indices, especially during solar minimum.

One advantage of the MG II index is that highly excited magnesium "exhibits the largest natural solar irradiance variability above 240 nm. It is [therefore] frequently used as a proxy for spectral solar irradiance variability associated with the 11-yr solar cycle" **[2]**. Yet, "while 280 nm is above the

204 nm wavelength that drives atmospheric photochemistry, the solar irradiance drops [only] about 4% from its average level for 1979 to 1983 measurements" **[9]**. In other words, the MG II index provides an accurate and reliable measurement of the EUV energy that most affects Earth's ionosphere, even though it is found within the ultraviolet (UV) portion of the electromagnetic spectrum.

In 2013, five commonly used solar proxies were compared, based on data collected from 1995 to 2010 **[7]**. This time span included the previous two solar minima and was comprised of the SFI (F10.7), Sunspot number (Rz), MG II index, Lyman-α intensity, and SEM EUV (304A) measurements. The hydrogen-produced Lyman-α spectral line is found at a wavelength of 121.6 nm and appears as the strongest single line in the EUV spectrum. It suffers from having been observed through a number of different instruments over the years, which introduced calibration errors. Calibration errors persist for all measurements of single spectral line intensities (amplitudes), since each instrument is characterized by its own gain. The same holds true for measurements of the helium 304A (30.4 nm wavelength) EUV measurement, provided by the SOHO (SEM) and SDO (EVE) satellites **[10]**. Furthermore, SOHO's measurements of 304A degraded over time when compared to SFI **[11]**. Unlike the other measurements cited in this study, the MG II index represents a ratio of absorption to emission spectra in the vicinity of 280 nm — referred to as the core-to-wing ratio (MGII c/w), which has the advantage of being "fairly easy to measure and relatively insensitive to instrumental artifacts" **[12]**. This allowed a reliable reconstruction of solar irradiance using the MG II index dating back to 1978 and continues to be updated daily **[2]**.

3 – Data Comparison for Amateur Radio Use

In order to confirm that the MG II index indeed acts as a proxy for solar irradiance (and shortwave radio propagation), I plotted the index together with SFI on the same chart (**Figure 2**). The SFI is shown in the lower trace (blue), while the MG II index is shown in the upper trace (red). The visual correlation suggests good agreement over the past four solar cycles. However, careful inspection of the two curves reveals significantly greater variability in the MG II index values during solar minima. Note also the uptick in the MG II index values at the very right side of the graph (most recent data).

Limiting the SFI and MG II index data to the year 2020 yielded the chart in **Figure 3**. The SFI decreased over this period from an average of 75 to between 69 and 70, and remained flat until the beginning of June, 2020. Meanwhile, the MG II index decreased to a minimum about mid-February and began to rise linearly throughout the remainder of this period. It was in the middle of this upward trend that the author (and others) noticed significant improvements in HF propagation, especially in the 10 m to 20 m band.

During the period of upward trending MG II measurements, several *plage* events

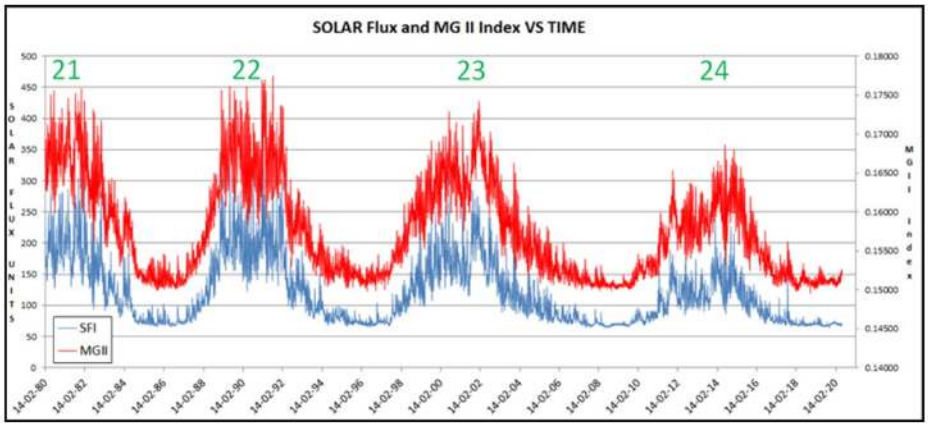

Figure 2 — SFI (lower trace) and MG II Index (upper trace).

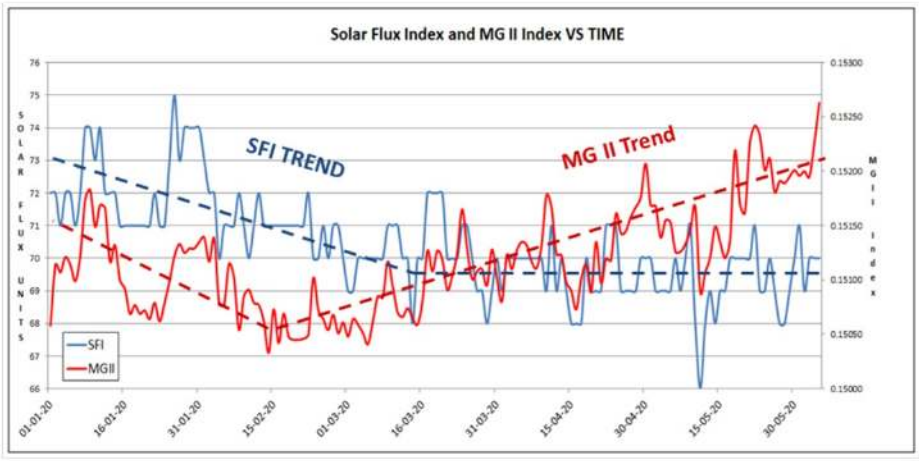

Figure 3 — SFI and MG II Index *vs.* time in 2020.

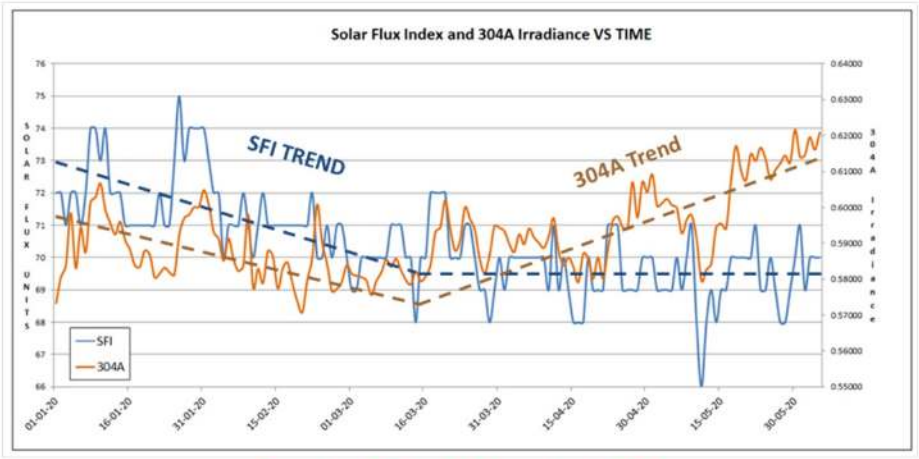

Figure 4 — SFI and 304A *vs.* time in 2020.

were in evidence in the EUV displays from the SDO. Starting as small but numerous regions, they became larger and brighter, culminating in the largest Cycle 25 Sunspot seen to date (active region 2765). This corresponded with the jump in the MG II index at the right hand side of the graph. At this time, it was reported that there were a number of good DX band openings in the higher frequencies of the HF spectrum (personal communications).

While researching the MG II index as a better proxy for shortwave radio propagation, the more commonly published EUV Helium 304A index (30.4 nm) was also compared to the solar flux index (**Figure 4**). Similar to the MG II index, the 304A data increased in intensity towards the later part of the spring, however this upward trend began about a month after the MG II index trend, and also showed less variability. Thus, both the 304A and the MG II index data could serve as better proxies for solar activity than SFI, yet the MG II index data appeared to contain greater variability and also corresponded more closely to periods of noticeable improvements in shortwave radio propagation.

4 – Conclusions

It was demonstrated that during solar minima, that commonly used indicators — such as Sunspot number and solar flux index — lack sufficient resolution to provide reliable forecasts of solar weather for amateur radio purposes. By contrast, the MG II index shows significantly increased sensitivity to subtle changes in the Sun's UV and EUV irradiance. The MG II index is aptly suited to fill in the gaps during times when the Sun's output is low. Other popular spectral intensity measurements, such as the single line emissions from Helium 304A and Hydrogen Lyman-α correlate well with the MG II index, but suffer from instrumentation issues over time. With the MG II index calculated as a ratio of absorption to emission in the vicinity of 280 nm wavelengths, instrumentation is less of a concern. The fact that this index provided an explanation to the enhanced "DX openings" during a period where these were unexpected, suggests that it worthy of inclusion in the propagation forecasting toolbox.

As a potential follow-up to this paper, it would be interesting to mine the PSK Reporter [4] database of digital signals (FT8, WSPR, etc.) for indications of improved DX communications ("band openings") and to attempt to correlate these events with local peaks in the MG II index values during the current solar minimum. Whether or not the minimum value of the MG II index corresponds to the transition between Solar Cycles 24 and 25 (mid-February, 2020 as seen in Figure 3) remains to be seen. Furthermore, as Cycle 25 begins its upward trajectory towards solar maximum, the MG II index may play a lesser role, but it may still yield some pleasant surprises in terms of enhanced day-to-day propagation predictability. Contesters, DXers and DXpeditions often rely on propagation forecasts, and having a better predictive tool will certainly be appreciated.

Jerry Spring, VE6TL, became a ham radio operator at the age of 16, in 1973, receiving his first call sign, VE3HCN, in Windsor, Ontario, Canada. After obtaining a B.Sc. (Physics) from York University in Toronto, Ontario in 1980, he spent the next 36 years working as a professional exploration geophysicist (P.Geoph.), searching for oil and gas domestically as well as internationally. This included postings in Texas, Indonesia, Australia, and Argentina before returning to Calgary in 1999 and retiring in 2016. In 2004, he rediscovered ham radio and has since obtained his 5BDXCC certificate and DXCC Challenge plaque. In 2009, he published the popular book "Hogwash for Hamsters" that features all original humor. His varied interests in ham radio include DXing, contesting, propagation forecasting, solar physics, restoring vintage radios, Arduino, electronic circuit design, teaching basic and advances licensing classes, and Elmering.

References

[1] UVSAT – UV satellite data and science group, University of Bremen; **www.iup.uni-bremen.de/UVSAT/Datasets/mgii**.

[2] F. S. Johnson, J. D. Purcell, R. Tousey, and N. Wilson, "A New Photograph of the MG II Doublet at 2800 A in the Sun," *Astrophys. J.* 117, 238-239. (1953).

[3] Solar Dynamics Observatory, (2020); **https://sdo.gsfc.nasa.gov/**.

[4] *PSK Reporter* Digimode Automatic Propagation Reporter (2020); **www.pskreporter.info**.

[5] *DX Maps* QSO/SWL real time information (2020); **www.dxmaps.com**.

[6] LiBo Liu, WeiXing Wan, YiDing Chen, and HuiJun Le, "Solar activity effects of the ionosphere: A brief review," *Chinese Science Bulletin*, Vol. 56, No. 12: 1202-1211, (2010).

[7] S. C. Solomon, L. Qian, and A. G. Burns, "The anomalous ionosphere between solar cycles 23 and 24," *J Geophys Res Space Physics*, Vol 118, 6524-6535, (2013).

[8] P.C. Anderson and J. M. Hawkins, "Topside ionospheric response to solar EUV variability," *J Geophys Res Space Physics*, 121, 1518-152, (2016).

[9] D. F. Heath and B. M. Schlesinger, "The Mg 280-nm doublet as a monitor of changes in solar ultraviolet irradiance," *J Geophys Res Atmospheres*, Vol. 91, Issue D8, (1986).

[10] *Science on a Sphere*®: NOAA (2020); **https://sos.noaa.gov/datasets/sun-helium-wavelength-aia-304/**.

[11] J. Spring), 1996-2012 Comparison of SoHo SEM 304A Data to SFI (2013); **www.hamqsl.com/solar2.html#images**.

[12] M. Snow, M. Weber, J. Machol, R. Viereck and E. Richard I., "Comparison of Magnesium II core-to-wing ratio observations during solar minimum 23/24," *J Space Weather Space Climate*, Vol 4, A04, (2014).

Peter DeNeef, AE7PD

2033 Abby Gate Dr., Roseville, CA 95747; **hamradioandvision@gmail.com**

RF Exposure Safety for a 70 cm Band Collinear Dipole Array

FCC regulations specify that radio amateurs comply with RF exposure limits, like on this collinear array

FCC regulations specify maximum permitted RF exposure limits. These limits determine compliance distances — the minimum separation between an antenna and persons in the surrounding area [**1, 2**]. I calculated compliance distances for a collinear dipole array, a high-gain amateur radio antenna for the 70 cm band.

As shown in **Figure 1**, the vertical array is comprised of four half-wave dipoles [**3**]. The feed points are spaced one wavelength apart, and the dipoles are driven in-phase. The overall length is 7.6 ft, and the center of the antenna is 9.7 ft above average ground.

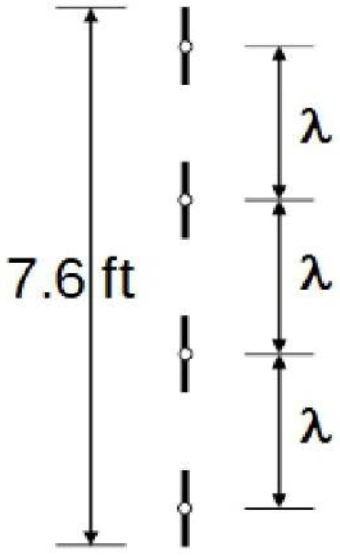

Figure 1 — *EZNEC* model of the 445 MHz collinear dipole array. Wavelength λ = 2.2 ft (0.67 m).

Figure 2 shows the free space vertical-plane pattern at 445 MHz. The maximum linear gain is $G = 7.29$ (8.63 dBi). My *EZNEC* [**4**] computer model is described on the *QEX* files web page [**5**].

Compliance Distance Formula

The easiest way to estimate compliance distances is with a simple formula that includes the effects of ground reflections. The compliance distance is,

$$D = 1.48\left(\frac{PG}{S}\right)^{1/2} \quad (1)$$

where D, ft, is the distance from the center of radiation, P, W, is the average power, G is the free-space power gain, and

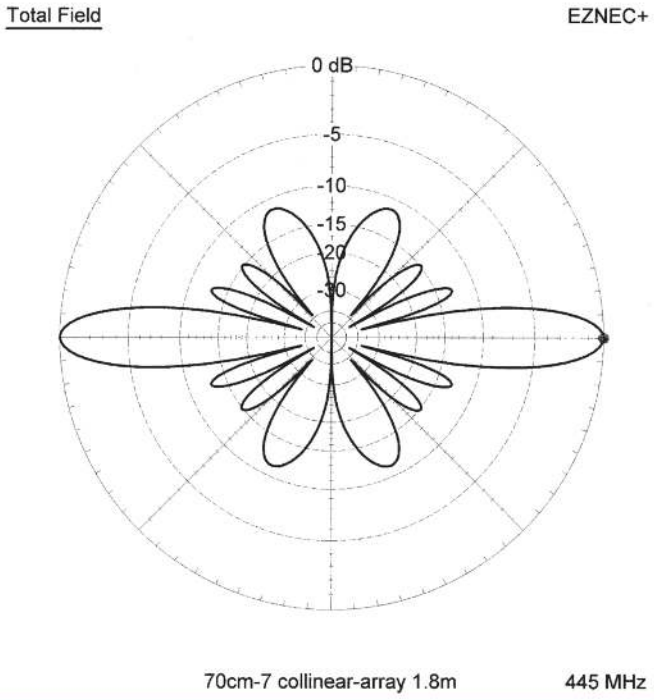

Figure 2 — Free space vertical-plane pattern at 445 MHz for the collinear array. The maximum power gain is 7.29 (8.63 dBi).

S, W/m^2, is the maximum permissible power density. This is Eq. (5.9) in **[2]**, revised to show S in W/m^2. The FCC refers amateurs to explanations of how to use the formula and tables of compliance distances **[1, 2]**. You can also use an online calculator **[6]**.

FCC regulations specify two different power density limits at each frequency. One is for *controlled* environments, where persons are aware of the potential for RF exposure and can take steps to limit the exposure. Limits for *uncontrolled* environments, where persons are not aware of potential exposure, are lower. At 445 MHz the FCC limits are 14.8 W/m^2 (controlled) and 3.0 W/m^2 (uncontrolled) **[1, 2]**. Controlled environment guidelines apply to amateur radio operators and members of their household. FCC regulations specify 6 minutes averaging time for the power in controlled environments and 30 minutes averaging time for uncontrolled environments.

Eq. **(1)** is based on the worst-case power density in the *far* field of the main beam. Estimates of *near* field levels using this model require validation. Computer simulations by the ARRL show that Eq. **(1)** gives conservative estimates of compliance distances for a wide range of dipole, ground-planes, and Yagi antennas used by amateurs **[1, 2]**. The formula underestimates compliance distances for some other antennas, including small transmitting loops and electrically short non-resonant wires **[7]**. These and other unusual antennas require additional evaluation.

The line in **Figure 3** shows *controlled* compliance distances *vs.* average power, calculated using Eq. **(1)** for the collinear array at 445 MHz. Distances in feet are measured from the center point of the array. Data points show calculations using *EZNEC* simulations that are described on the *QEX* files web page **[5]**. These distances are measured horizontally between the antenna axis and the point of exposure. **Figure 4** shows *uncontrolled* compliance distances *vs.* average power. Both figures show that Eq. **(1)** overestimates the *NEC* (Numerical Electromagnetic Code) distances.

For a comparison, I used Eq. **(1)** to calculate compliance distances for a ground-plane quarter-wave monopole with four 45° radials. The connection point for the five elements is 5.9 ft above average ground. The *EZNEC* model is described on the *QEX* files web page **[5]**. **Figure 5** for controlled areas and **Figure 6** for uncontrolled areas show that compliance distance estimates from the formula are less restrictive (closer to the *NEC* calculations) than the results for the collinear dipole.

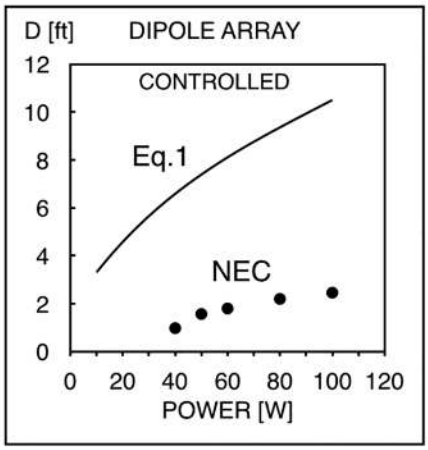

Figure 3 — Controlled compliance distance D [ft] *vs.* average power P [W] at 445 MHz for the collinear array. The line shows estimates from Eqn (1). Data points show NEC calculations for center height of 9.7 ft.

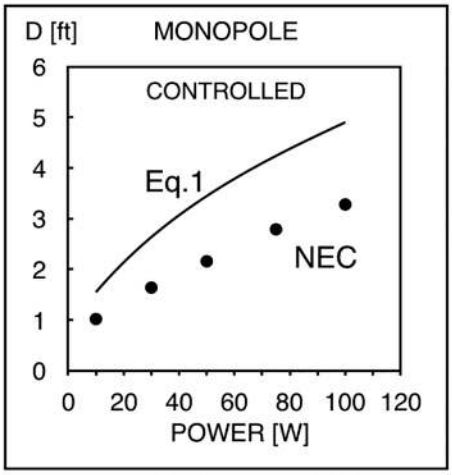

Figure 5 — Controlled compliance distance D [ft] *vs.* average power P [W] at 445 MHz for the quarter-wave monopole. The line shows estimates from Eqn (1). Data points show NEC calculations for center height of 5.9 ft.

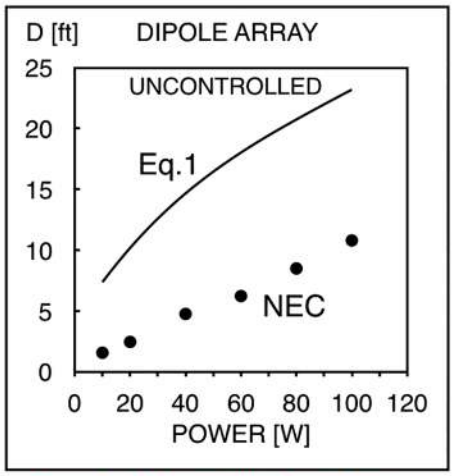

Figure 4 — Uncontrolled compliance distance D [ft] *vs.* average power P [W] at 445 MHz for the collinear array. The line shows estimates from Eqn (1). Data points show NEC calculations for center height of 9.7 ft.

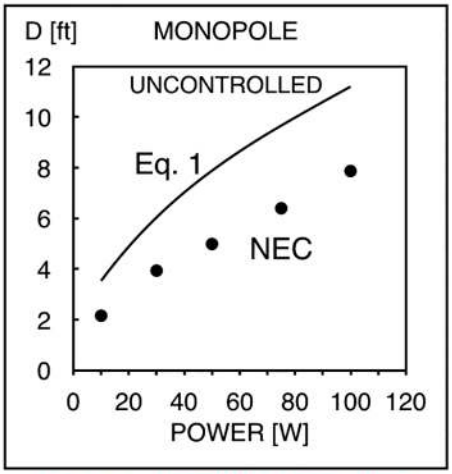

Figure 6 — Uncontrolled compliance distance D [ft] *vs.* average power P [W] at 445 MHz for the quarter-wave monopole. The line shows estimates from Eqn (1). Data points show NEC calculations for center height of 5.9 ft.

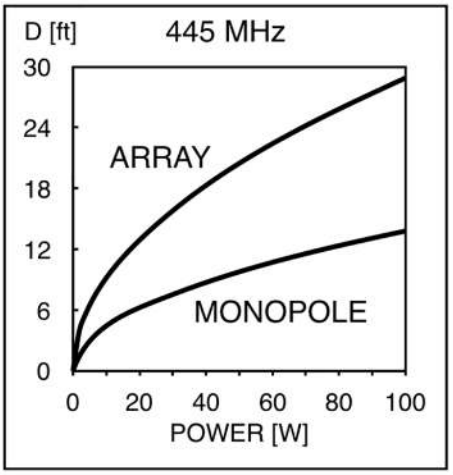

Figure 7 — New thresholds for station evaluation at 445 MHz for the collinear array (upper line) and quarter-wave monopole (lower line). P is the 30 minute average power [W], D [ft] is the separation distance between the center of radiation and point of exposure.

Required Station Evaluation

The power threshold for routine evaluation of amateur radio stations depends on frequency. For the 70 cm band, longstanding FCC regulations require evaluation if the peak envelope power (PEP) exceeds 70 W **[1, 2]**.

Table 1
NEC calculations of the horizontal distance in feet from the 445 MHz collinear dipole array to comply with controlled or uncontrolled exposure limits. The center height of the array is 20 feet. "0 feet" indicates that the exposure at the height indicated is in compliance everywhere in that horizontal plane.

Average power, W	*6 ft height, con.*	*6 ft height, unc.*	*12 ft height, con.*	*12 ft height, unc.*	*20 ft height, con.*	*20 ft height, unc.*
10	0	0	0	0	0	2
25	0	0	0	0	0.5	2.5
50	0	0	0	0	2	3
100	0	0	0	0	2.5	12
200	0	0	0	0	3	19.5
250	0	0	0	0	3	23
300	0	0	0	0	3.5	24
400	0	0	0	4	9.5	29
500	0	0	0	4.5	12.5	30.5
600	0	0	0	4.5	13	34.5
750	0	0	0	5	16	38.5
1000	0	7.5	0	5	19.5	46
1250	0	8.5	0	9.5	23	48.5
1500	0	9	0	10	24	56.5

The FCC recently amended the RF safety rules with new power thresholds for evaluating amateur radio stations. All amateur radio operators are required before May 31, 2022, to determine if an RF safety evaluation is required under the new criteria and, if indicated, to complete an evaluation [**8, 9**].

For base-station antennas there are two criteria for exemption from further evaluation:

1) All points where RF exposure can occur must be outside the reactive near field region. The separation distance D measured from any point on the antenna must be greater than $\lambda/2\pi$, where λ is the free-space wavelength. At 445 MHz, $\lambda/2\pi$ is 0.11 m (4.3 inches); and

2) The effective radiated power (ERP), must be no higher than the frequency-dependent thresholds (page 26 in [**8**]). ERP is defined relative to a half-wave dipole: ERP = $(PG)/1.64$, where G is the power gain of the antenna, and 1.64 is the power gain of a half-wave dipole. For this purpose P, W, is the average power to the antenna, averaged over any 30 minute time period.

Figure 7 shows the new thresholds at 445 MHz for the collinear array (upper line) and the quarter-wave monopole (lower line). When a separation distance D is closer to the antenna than the threshold distance for a chosen power P on the graph, assessment of RF exposure is required. For example, at 50 W average power, a compliance evaluation is required when the point of exposure is within 20 feet of the collinear array. For the quarter-wave monopole the threshold is 10 feet.

Repeater Antennas

Repeater antennas are subject to different exemptions from evaluation, see pages 3 to 4 in **[1]**. For building-mounted antennas, evaluation is required for amateur repeater stations transmitting with radiated power greater than 500 W ERP. For antennas mounted on stand-alone towers, evaluation is required if the height above ground level to the lowest point of antenna is less than 10 m and the power is greater than 500 W ERP.

Table 1 shows my *NEC* calculations of compliance distances for a collinear dipole array when the center height is 20 feet above average ground. The data are presented in the same format as the ARRL *NEC* tables **[2]**, showing average power and distances for compliance at three exposure heights — 6, 12, and 20 feet.

At the highest power levels in the table the uncontrolled compliance boundary extends down to the 6 foot elevation level.

Conclusions

Although the collinear dipole array is a high gain antenna, near field levels and NEC compliance distances are comparable to a quarter-wave monopole. Eq. (1) gives reasonable, conservative estimates of compliance boundaries for many common types of antennas, but estimates for the collinear dipole are overly conservative compared to NEC compliance boundaries.

For increasing antenna gain the new FCC base-station evaluation thresholds become more restrictive, requiring evaluation at lower power.

My thanks to Steve Stearns, K6OIK, for his helpful comments.

Peter DeNeef, AE7PD, received his first license KF7FPX in 2009. He has written about RF exposure safety for QEX, *as well as articles about international RF safety guidelines of the International Commission on Non-Ionizing Radiation Protection (ICNIRP). More of his articles can be found on his popular web site for vision-impaired hams,* **www.HamRadioAndVision.com**.

References

[1] Evaluating Compliance with FCC Guidelines for Human Exposure to Radiofrequency Electromagnetic Fields, OET Bulletin 65b (1997); **https://www.fcc.gov/bureaus/oet/info/documents/bulletins/oet65/oet65b.pdf**.
[2] E. Hare, W1RFI, "RF Exposure and You," ARRL, 1998, reprinted 2003. Archived at **www.arrl.org/rf-safety-publications**.
[3] *Antenna Book, 21st Edition*, ARRL, 2007-8, pp. 17-5 to 17-7.
[4] *EZNEC* antenna modeling software by Roy Lewallen, W7EL; **www.eznec.com**.
[5] QEXfiles; **www.arrl.org/QEXfiles**.
[6] P. Evans, VP9KF, Amateur Radio RF Safety Calculator; **hintlink.com/power_density.htm**.
[7] P. DeNeef, AE7PD, "RF Exposure Safety with Three Multi-Band Inverted L Antennas," *QEX*, Nov./Dec. 2017, pp. 3-5.
[8] Proposed Changes in the Commission's Rules Regarding Human Exposure to Radiofrequency Electromagnetic Fields, FCC 19-126, Dec. 4, 2019, pp. 25-6; **https://docs.fcc.gov/public/attachments/FCC-19-126A1.pdf**.
[9] Proposed Changes in the Commission's Rules Regarding Human Exposure to Radiofrequency Electromagnetic Fields, FCC 13-39, Mar. 29, 2013, pp. 123-6; **https://docs.fcc.gov/public/attachments/FCC-13-39A1.pdf**.

Eric P. Nichols, KL7AJ
AlasKit Educational and Scientific Resources, 3763 Lyle Ave., North Pole, AK 99705; **kl7aj72@gmail.com**

Self-Paced Essays — #5 Electromechanics and Control Systems

Essay 5: Electromechanical devices like motors and solenoids, and their control, play an important role in amateur radio.

For many modern day radio amateurs raised in the era of microprocessors and smart phones, "primitive" devices like motors and solenoids might seem boring. However, as I have learned — along with a number of other radio amateurs — it is always helpful to review the basics. Electromechanical devices have evolved tremendously in the past few years, with the development of ever more advanced robotic controls available to radio amateurs and other experimenters. See my November, 2014 *QST* article, "Motors and Mechanisms in the Ham Shack."

There is a whole branch of science and engineering known as *control theory*, that most hams only brush up against, or manage to avoid entirely, since it is primarily associated with the aforementioned "boring" electromechanical or mechanical devices. However, one of the important concepts that one learns in studying electromechanical devices is that the universe is remarkably consistent. We can understand electrical circuits by using mechanical analogies in a great number of cases. For instance, we can use simple *plumbing* concepts to fully demonstrate electrical principles such as Kirchhoff's Current Law. Likewise electromechanical control concepts can apply directly to electronic *oscillators*. Whether we're dealing with mechanical, acoustic, or electrical devices, nearly all the math is identical.

Until fairly recently, *control theory* was fairly informal, only really becoming a concrete discipline after World War II. My father, John B. Nichols, was actually a pioneer in this field; he held the original patent for automatic helicopter rotor speed control — US Patent 3,049,178, "Helicopter Governor." Just to illustrate how basic and wide-ranging this patent was, it's only three pages long! If this were applied for today, it might be *hundreds* of pages long. There really weren't any serious competitors in this field at that time. Incidentally *Silicon Valley*, where this helicopter system was patented, was a high-tech hub of aviation and aerospace long before it was an electronics hub.

Stability

One of the most important characteristics of any control system, whether it's electrical, electronic, electromechanical, or a combination of the above, is *stability*. Does the device or system do what you want it to do each and every time you ask it to do it, and without any undesirable side-effects? Often, this is a lot easier said than done. But let's explore one simple mechanical concept that can be applied in many other devices.

Shock Absorbers

If you are, or ever were any kind of a gear head, you probably learned a simple way of testing out a car's shock absorbers. You stood on the car's bumper, and jumped off. If the shock absorber was doing its job, the bumper would pop up just slightly beyond the neutral point and immediately settle down to its normal height. What you were doing, whether you had a name for it or not, was looking for a condition known as *critical damping*. If the shocks were bad, the front (or rear) of the car would continue bouncing up and down. This is known as an *under-damped*, condition, which can result in a very *unstable* ride. You don't want the car to continually bounce up and down after hitting a bump. On the other hand, if the shock absorber is the wrong type (too big, for instance), the system would be *over-damped*, resulting in a somewhat harsher ride. In theory, with an over-damped shock absorber/spring combination, the bumper height would never return to its neutral height, but only approach that height *asymptotically*. In reality, you would probably never encounter a shock absorber with *infinite* recovery time.

Mechanical Oscillators

A car body (or a corner of it) bouncing up and down on a spring is an *oscillating* system. The oscillator consists of two components, the mass of the vehicle and the spring. If no shock absorber were present, and there were no air resistance or friction in the spring, the car would bounce up and down forever in a perfectly sinusoidal fashion. The frequency of the oscillation would depend only on the stiffness of the spring and the mass of the car body. To be really persnickety about the situation, the oscillation is not *perfectly* sinusoidal, because the acceleration of gravity is constant, while the acceleration imparted

by spring is proportional to its displacement (according to Hooke's Law), but we can ignore this error for now.

In the absence of friction (resistance), there is no loss of energy. The energy is merely transferred between two forms of energy: kinetic energy (the motion of the vehicle's body) and potential energy (compression of the spring). Assuming our shock absorber is the only source of resistance, we will find that all the stored energy is eventually converted into heat in the shock absorber. If we have the *right* shock absorber, we will find all the energy converted into heat after one oscillation of the bumper. Again, this is our *critically damped* condition.

The Q of Everything

A critically damped system is one in which the dissipated energy is well-matched to the stored energy. In mathematical terms, we state that the critically damped system has a Q of ½. We will refer to this all-important Q factor many times throughout this series. Electrically speaking, Q is equal to X/R, where X is the reactance or energy storage property of the system and R is the resistance or *friction* of the system (see K. Siwiak, KE4PT, "Q and the Energy Stored Around Antennas," *QST*, February, 2013). Q is a *dimensionless* quantity. But this in no way diminishes its importance in all things electrical or mechanical. In most radio circuits we work with *much much* higher values of Q than in our critically damped system, where we often *want* sustained oscillations. We'll talk a lot more about the subtleties of Q in the months to come. The important thing is to realize that mechanics and electronics both live in the same universe and use the same mathematics.

Working Things Out

Another all-important concept that seems to be hidden in radio electronics is the concept of *work*. We don't normally think of a radio — or even a computer — as something performing any real mechanical work. We relegate that idea to things like generators, or maybe antenna rotators. But ultimately, no matter how feeble a radio signal may seem, the ultimate goal of all our elaborate electronics is to produce real mechanical work, even if that only involves vibrating a loudspeaker, which in turn wobbles some air, which in turn wobbles our eardrums.

So, let's address some crude, perhaps barbaric-seeming concepts in the mechanical world and apply them to our delicate, sophisticated, electronics domain.

Work is defined qualitatively as force applied times distance moved. If we want to scoot a shipping crate across the floor, we can measure the force it takes to move the thing, and multiply that by the distance we've moved it, and come up with a figure in something like pound-feet. This, naturally, assumes the same amount of friction and speed throughout the travel of the shipping crate. Things are a bit more complicated when we consider the *acceleration,* if any. Work is *dimensionally equivalent* to energy. If we figure out the amount of calories we burned in scooting the crate across the floor, we can replace pound-feet with calories or joules. We will work with very many *dimensionally equivalent* values in our essays, so it's a good idea to become familiar with the manipulation of these values.

Now, since we are primarily *electrical* folks, we will be using mainly an electrical unit of energy, namely the joule (J) or the watt-hour (Wh). Your friendly local power provider will probably not bill you for calories burned, although the watt-hour and the calorie *are* dimensionally equivalent. In case you really need to know, there are 860.421 calories per watt-hour.

Now, we've taken a big lap around the field just to come back to our original point that *energy* is all-important. Energy comes in two essential forms, stored energy and dissipated energy. The design and maintenance of any kind of control system involves the proper use and proportioning of stored and dissipated energy. If you take the time and energy — pun intended — to allow these two basic concepts to really sink in, so many electronic concepts will become very intuitive.

What is Control?

As indicated earlier, wherever possible, we will use familiar mechanical analogies to describe obscure electrical principles.

When we think of control, we normally think of some small cause (or *signal*) making some larger effect take place. One way of describing this is *amplification of intent*. If you're an equestrian, you can convey your intentions to a very large horse by means of a very subtle signal transmitted by the reigns.

Another example is the valve on top of a fire hydrant. With relatively small effort, one can cause a very large, high pressure stream of water to turn on or turn off. A water valve is an *amplifier of intent* in this application. It is no accident that the British use the term *valve* for what Americans call a vacuum tube, the oldest electrical amplifying device.

Modern electromechanical control systems can use combinations of electrical and mechanical amplification to achieve finely-tuned control over the final results. The *servomechanism* is an important class of devices using mechanical and electrical amplification and feedback to achieve precise speed, position, or acceleration of some physical device.

Although feedback — specifically *negative* feedback — is an important facet of most modern control systems, it is not necessary to have feedback in every well-controlled system. Although negative feedback is sometimes credited with covering a "multitude of sins" it can also create some original ones as well! We will delve into this in more detail as we move through this series.

Switching Things Up

While most of the mechanical devices we've touched on in this essay are *analog* in nature, we can't ignore the simplest *digital* device in this discussion: the electrical switch. There's a lot to be said about making switches behave as they should. They don't get anywhere near the attention they deserve in the typical amateur radio installation. Since the electrical switch — and its close cousin, the *relay* — are likely the slowest responding components in any modern electronic or radio system, they can have the most profound effect on the overall performance. No switch is perfect, even if we disregard the speed factor. Switch contacts have finite resistance. They are also subject to dynamic effects such as *contact bounce*, which can have all kinds of baffling effects in more complex systems.

In Summary

This has been a bit of a side trip off the beaten path of normal electronics, but we trust it has been enlightening; again, we can't over-emphasize how consistent our physical universe is. Soon, we will take another side trip into some *chemistry*, just to stir things up a bit. Again, we will find some astonishing and comforting consistency in our universe — a nice contrast to our current world-wide chaos!

Technical Notes

Lightning-Induced EMP

Is it possible for lightning to get into your rig in the absence of a direct conductive connection? The surprising answer is maybe! We make a crude estimate here of the order of magnitude of that effect.

A conductive path is not the only way that lightning can cause havoc with your amateur radio station. There are also inductively and capacitively coupled paths, sometimes called lighting-induced electromagnetic pulse (L-EMP). The lightning bolt conducts a transient current that gives rise to a magnetic field surrounding the bolt from the blue. That magnetic field can then couple inductively to a loop of wire at your station, and generate potentially damaging voltages at your station. If oriented for maximum coupling, the lightning bolt having an peak current I_B will induce a peak voltage V_{MAG} in ends of a loop of wire D_B meters away. From Faraday's Law of induction, and after some manipulation,

$$V_{MAG} = \frac{-N\mu_0 r^2 I_B}{2D_B t_D}$$

where $\mu_0 = 4\pi \times 10^{-7}$ H/m, N is the number of turns in the coiled up wire loop, r is the loop radius, and t_D is the rise time of the bolt current.

Considering the inductive coupling, a 90th percentile strike — with a peak current of 200,000 A, a current rise time of 5 µs (the decay time is in the 50 to 100 µs range), 10 m away — will induce a transient peak of about V_{MAG} = 630 V in the ends of a one-turn 0.5 m radius loop of wire, or in a 10-turn bundle of wire 0.16 m in radius (1 ft diameter)!

Close by, there is also a corresponding transient radial electric field $E = v(t)/D_B$ between the bolt channel and a parallel length of wire D_B meters away, which can couple a current $i(t)$ capacitively over a short distance. A simplistic model of this mechanism is,

$$i(t) = C\frac{dv(t)}{dt}$$

where C is the mutual capacitance between the lightning bolt and the length L of wire, which to first order can be estimated from an equivalent parallel transmission line of D_B separation between the bolt channel, and an L m length of a parallel conductor. We take ΔV to be the 3 MV/m dielectric breakdown of air, the lightning strike can induced a peak current,

$$I_{PEAK} = \frac{\pi\varepsilon_0 \Delta V L}{\ln\left(\frac{D_B}{a_{TL}}\right) t_D}$$

in an L meter long straight conductor, where a_{TL} is the radius of both the conductor and the lightning channel. The model is far from perfect, but predicts that for a_{TL} = 0.005 m, the mutual capacitance works out to be a few pF, and we get I_{PEAK} = 4.4 A in an L = 2 m long conductor that is D_B = 10 m away.

These threats to your station might be hidden in a bundled-up coil of Ethernet cable, or other bundled-up power or audio cables, or even a loop of grounding wires in your shack! To combat this threat, your station should not have any wires, including grounding wires, that inadvertently form loops, or that are not grounded. When you coil-up excess cables or wires, squash the loop bundle in the middle with a single twist, or bundle it up in figure-8 fashion.

I lost the audio section (no other damage) of my Icom IC-706mkIIg because it was connected to *nothing other than a bundled-up loop of audio cable* going to an external speaker. The bolt struck a grounded **J** pole antenna mast just a few meters away from the shack.

As a matter of curiosity, L-EMP can have other surprising effects. The peak magnetic field H_B wrapping around a vertical lightning bolt strike with peak current I_B is,

$$H_B = \frac{I_B}{2\pi D_B} \text{ A/m.}$$

If at a far enough distance, a corresponding vertical electric field magnitude were $E = 376.73|H_B|$ V/m, then the absorption electromagnetic radiation pressure normal to the bolt is (with c = speed of light),

$$P_{rad} = \left|\frac{376.73 H_B^2}{c}\right| \text{ Pa.}$$

That 200,000 ampere bolt *50 meters away* would result in a pressure of 0.5 Pa (compared with the 3.3 µPa absorption radiation pressure at the Earth's surface from the Sun), or the sudden application of a 1.6 ounce spike of physical pressure. That's the weight of a dozen QSL cards distributed over, say, the half-surface of your body. That's not much, but it's not zero; and I would imagine that the associated thunderclap will likely be more startling than the radiation pressure! — *With kindest regards, Kai Siwiak, KE4PT,* **k.siwiak@ieee.org**.

Upcoming Conferences

Virtual 2021 SARA Spring Conference

April 2, 2021

www.radio-astronomy.org

The 2021 SARA Spring Conference will be held on Zoom, April 3, 2021. This virtual conference will replace the annual SARA Western Conference because of the continuing COVID-19 pandemic.

Please contact conference coordinator Dave Westman if you have any questions about the conference or if you would like to help: **westernconf@radioastronomy.org**.

Registration for the 2021 Spring Conference is just US$25.00. Attendees at the conference must be SARA members; if you are not yet a member, this will cost an additional $20. See website for details.

Central States VHF Society Conference

July 30 – 31, 2021
(postponed from July 2020)

La Crosse, Wisconsin

www.2020.csvhfs.org

The 54th annual Central States VHF Society Conference will be held at the Radisson Hotel located on the beautiful riverfront of the Mississippi River in La Crosse, Wisconsin on July 30 – 31, 2021.

Check website for details.

Digital Communications Conference (DCC)

September 17 – 19, 2021

Charlotte, North Carolina

www.tapr.org

The 40th annual ARRL and TAPR Digital Communications Conference (DCC) will take place September 17 – 19, 2021 in Charlotte, North Carolina at the Hilton Charlotte Airport Hotel, 2800 Coliseum Centre Dr., Charlotte, NC 28217.

Details for DCC and hotel registration will appear on the website as soon as they are available. In the meantime, it is not too early to plan technical papers and presentations for the event.

DX Engineering—Your Source for the Icom IC-705 and Accessories!

ICOM

Icom IC-705 HF/50/144/430 Portable Transceiver

With the features and functionality of the IC-7300, IC-7610, and IC-9700, Icom's new QRP rig is like owning a base transceiver you can hold in one hand. It boasts SDR Direct Sampling technology for stellar transmit and receive performance; 4.3" color touchscreen; real-time spectrum scope and waterfall display; built-in Bluetooth®; wireless LAN; and full D-STAR capabilities. **Enter "IC-705" at DXEngineering.com for details and user reviews.**

ON ALL BANDS

DX Engineering's Amateur Radio Blog for New and Experienced Hams.

ICOM

Mounts and Stands

Choose from the BASE-705 Desk Stand from WiMo, featuring a flat steel plate for stability in the field or the shack; WiMo's MBA-705 Holder with Antenna Mount, which allows for convenient mounting of an antenna and counterpoise; Icom's MBF-705 Desktop Holder; and the Heavy-Duty IC-705 Desk Stand from Nifty. **Enter "IC-705 Stand" at DXEngineering.com.**

VIBROPLEX

Automatic Antenna Tuner

mAT-TUNER, a member of the Vibroplex family, introduces the MAT-705 PLUS. This handy device adds tuning functions to the IC-705, with the ability to tune dipoles, verticals, Yagis, or virtually any coax-fed antenna within the range of 1.8 MHz to 54 MHz. The unit boasts tuning times of 0.1 to 5 seconds full tune, 0.1 seconds memory tune. The PLUS version features a power supply that is automatically controlled by the transmitter. **Enter "MAT-TUNER IC" at DXEngineering.com.**

ICOM

Magnetic Loop Antenna

Designed by alpha antenna™ to optimize the performance of the IC-705 and other Icom rigs, this well-built antenna features band coverage from 40-10M. Maximum power is 20W SSB and 10W CW and Digital. The unit compacts down to 10" x 11" x 2.5" for convenient storage and transport in the IC-705 backpack (LC-192). Includes 25 feet of coaxial cable. **Enter "AL-705" at DXEngineering.com.**

ICOM

Backpack

Icom's LC-192 Portable Transceiver Backpack makes it easy to transport your IC-705 wherever your adventures take you! It features rugged nylon construction, specially-designed compartment with integral thumbscrew to secure the IC-705, lower compartment with ample storage space, reinforced side panel for mounting a portable antenna, and portals for speaker mic and antenna leads. **Enter "LC-192" at DXEngineering.com.**

Nifty! Ham Accessories

Manuals and Software

Nifty's IC-705 Mini-Manual may measure only 4.5" x 8", but its 26 laminated pages are loaded with detailed instructions, including clear descriptions for all controls, setup menus, and modes of operation. From RT Systems comes WCS-705 Programming Software, which makes it easy to manage memory channel information, D-STAR settings, and more. Package includes RT-49 cable. **Enter "Nifty IC-705" and "WCS-705" at DXEngineering.com.**

rt SYSTEMS
RADIO PROGRAMMING MADE EASY

YAESU ICOM KENWOOD AlexLoop COMET SB SOTABEAMS HEIL SOUND

Check Out DX Engineering's Facebook Page and YouTube Channel!

DX® ENGINEERING

Curbside Pickup Hours:
9 am to 8 pm, Monday-Saturday
9 am to 7 pm, Sunday

Ordering (via phone):
8:30 am to midnight ET, Monday-Friday
9 am to 5 pm ET, Weekends

Phone or e-mail Tech Support: 330-572-3200
8:30 am to 7 pm ET, Monday-Friday
9 am to 5 pm ET, Saturday

Email: DXEngineering@DXEngineering.com
All Times Eastern | Country Code: +1

800-777-0703 | DXEngineering.com

ON ALL BANDS YouTube

We're All Elmers Here! Ask us at: Elmer@DXEngineering.com
Email Support 24/7/365 at DXEngineering@DXEngineering.com

YAGI URBAN BEAM

The UrbanBeam is excellent for use in high density population areas or properties with small lot sizes, where a full-sized Yagi may not be an option. The distinctive shape and small footprint (15.5 sq ft turning radius) of the UrbanBeam helps make neighbors and spouses happier, while still delivering the exceptional results you would expect of a SteppIR Yagi. The UrbanBeam is a high-performance, two element Yagi on 20m-6m and folded dipole on 40-30m. With features such as 180 degree direction change, bi-directional mode and full element retraction for stormy weather. You can enjoy all the features of a SteppIR Yagi while chasing low-sunspot-cycle DX or rag-chewing with your friends!

YAGI URBAN BEAM

GO SMALL

steppIR COMMUNICATION SYSTEMS

DETAILS & ORDERING:

www.steppir.com

425-453-1910